TOPICAL REVIEW

Low temperature plasmas and electrosprays

To cite this article: Anatol Jaworek *et al* 2019 *J. Phys. D: Appl. Phys.* **52** 233001

IOP ebooks™

Bringing you innovative digital publishing with leading voices to create your essential collection of books in STEM research.

Start exploring the collection - download the first chapter of every title for free.

Topical Review

Low temperature plasmas and electrosprays

Anatol Jaworek[1] **, Alfonso M Gañán-Calvo**[2] **and Zdenko Machala**[3,4]

[1] Institute of Fluid Flow Machinery, Polish Academy of Sciences, ul. Fiszera 14, PL 80-231 Gdansk, Poland
[2] Depto. de Ingeniería Aeroespacial y Mecánica de Fluidos, Universidad de Sevilla, E-41092 Sevilla, Spain
[3] Faculty of Mathematics, Physics and Informatics, Comenius University, 84248 Bratislava, Slovakia

E-mail: machala@fmph.uniba.sk

Abstract

The paper reviews the state of the art in the field of interaction of low temperature plasmas generated during electrospraying with the liquid cone and jet. Many studies are focused at practical applications of electrospraying, for example to mass spectrometry, electrospinning of nanofibers, thin film deposition, nanoparticle production, ink-jet printing, etc, but the phenomenon of electrically generated plasma due to gas ionization accompanying the electrospraying is frequently ignored. The effect of electrical discharge on the electrospraying process depends on the type of the discharge. When glow corona or onset streamers are generated, the electrospray is stabilized in the classical cone-jet mode, however, for breakdown streamers, sparks, or arc discharges, the electrospraying process is disturbed and irregular modes (spindle, multispindle or ramified jet) occur. The electrospray-discharge interaction phenomena have been studied by photographic recording, electric current measurements, mass spectrometry and optical emission spectroscopy. Some studies show that the current carried by the ions generated in this plasma and flowing through the drift region to the opposite electrode can be higher than the current carried by the electrosprayed droplets. This effect has been proved by separation of both currents using a specially designed device. To prevent the distortion of the electrospray process, various strategies have been developed: modification of the electric field in the vicinity of capillary nozzle, stabilization of the glow corona, reduction of the surface tension of liquid. Recently, the physical processes and phenomena occurring in electrical discharge plasmas during electrospraying of liquids find new application in decontamination of liquids or in material processing. The advantage of the coupled electrospray-plasma process is that the liquid atomization is combined with plasma chemical processes within the same device, by using the same power supply applied to the capillary nozzle.

Keywords: electrostatic spraying, low temperature plasma, electrohydrodynamic spraying, EHDA, corona discharge, streamer discharge, glow corona, plasma activated water

(Some figures may appear in colour only in the online journal)

[4] Author to whom any correspondence should be addressed.

J. Phys. D: Appl. Phys. **52** (2019) 233001

Topical Review

1. Introduction

The electrohydrodynamic ejection of liquids, commonly known as electrospray phenomena, occurs when a strong electric field is applied to exposed liquid surface. The fundamental physical mechanism lays on the free charges present in the liquid when they are moved by an externally applied electric field and hit the free surface. The surface prevents them from reaching the counter electrode, and the charges accumulate and eventually form a charged layer at the surface in characteristic times comparable to the electrical permittivity of the liquid ε_l divided by its conductivity κ_l (known as the charge relaxation time $t_e = \varepsilon_l/\kappa_l$, Melcher and Taylor (1969); we give more details in subsequent sections). Since a liquid cannot stand a continuously applied stress unless it is non-Newtonian, the surface stresses provoked by the charge layer subjected to the applied electric field eventually induce the ejection of liquid towards the counter electrode.

Among the different forms of liquid ejection, the well-known steady Taylor cone-jet mode is a stable, steady ejection regime where electric and fluid stresses acting on the liquid with scales spanning several orders of magnitude find a delicate balance (that will be subsequently detailed) in the form of a liquid cone, and an extremely thin charged capillary jet is continuously ejected from the cone apex. In these steady conditions, the charge layer on the liquid surface nearly shields the liquid bulk from the externally applied potential difference. However, the local equilibrium of the surface stresses demands a first-order balance between the surface tension and the electric forces in the normal direction to the surface, which in turn requires very large surface curvatures when the charge density on the surface is large as well. In the cone-jet mode, these large curvatures and strong local electric fields occur at the jet, usually close to the cone-jet transition.

In the electrospraying of liquids from capillary nozzles, strong local electric fields appear not only at the jet. Due to a high electric potential applied to the nozzle and low radii of the capillary nozzle, meniscus and jet at the nozzle outlet, the electric field at the surface of those objects is often sufficiently high to cause the ionization processes in the surrounding gas (Jaworek (2014) and references therein). These processes are well known for electrical discharges from solid (typically metal) surfaces and were observed by many authors. Usually, this phenomenon is known as the *corona discharge*, when it occurs by a low discharge power at sharp edges of the nozzle where the electric field is locally enhanced. The problem of corona discharge from the surface of conducting liquids, including the liquid jet from the electrospray nozzle, or from a charged droplet, has also been investigated using various experimental tools (Zeleny 1914, 1915, 1917, 1920, Macky 1931, English 1948, Schultze 1961, Akazaki 1965, Dole *et al* 1968, Giao and Jordan 1968, Burayev and Vereshchagin 1971, Phan-Cong *et al* 1974, Hoburg and Melcher 1975, Bailey and Borzabadi 1978, Ballinger *et al* 1978, Ogata *et al* 1978, Hara and Akazaki 1981, Barber and Swift 1982, Yamashita and Fenn 1984, Joffre and Cloupeau 1986, Smith 1986, Hayati *et al* 1987a, 1987b, Meesters *et al* 1992, Straub and Voyksner 1993, Wampler *et al* 1993, Cloupeau 1994, Cloupeau and

Prunet-Foch 1994, Rosell-Llompart and Fernandez de la Mora 1994, Tang and Gomez 1995, Borra *et al* 1996, 1999, 2004, Jaworek and Krupa 1997, Cole 2000, Cech and Enke 2001, Gemci *et al* 2002, Ku and Kim 2002, Jaworek *et al* 2005, 2014, Stommel *et al* 2006, Bruggeman *et al* 2007, Korkut *et al* 2008, Jung *et al* 2009, Kim *et al* 2011, 2014, Pongrac and Machala 2011, Shirai *et al* 2011b, 2012, 2014, Elsawah *et al* 2012, 2013, Machala *et al* 2013, Pieterse 2013, Klee *et al* 2014, Pongrac *et al* 2014a, 2014b, 2016, Pieterse *et al* 2015, Kovalova *et al* 2016, Higashiyama *et al* 2017, Xu *et al* 2017). The results of these investigations proved that under certain conditions, especially for polar liquids, the ionization processes can occur close to the surface of the capillary nozzle— where the edges and corners are typically present—and of the jet, or in the interelectrode space. Numerical simulations of electric field distribution close to the surface of the nozzle and the jet confirmed that the magnitude of the electric field can be higher than 10^6 V m^{-1} (Jaworek *et al* 2016), which is sufficiently high for gas ionization.

In the case of electrospraying, the effect of corona discharge on the stabilization or disturbance of the electrospraying process, particularly in the cone-jet mode, is still an unresolved problem. This is an important question because of practical reasons. In technological applications, such as surface coating, microparticle and microcapsules production or jet printing (Jaworek *et al* 2018), uncontrolled discharges could hamper a stable electrospray operation for the production of monodisperse or controllably sized droplets. In that case, finding the effective means to control corona discharge are necessary to overcome these difficulties. Similarly, if the electrospray method is applied to the processing of biological or other fragile samples, for example in mass spectrometry, these samples could be damaged due to the bombardment by ions generated by electrical discharges, or due to chemical reactions with free radicals produced in the discharge.

Many publications reported that glow corona discharge is an intrinsic property of electrospraying, when the dripping mode changes to another electrospraying mode with the voltage increasing (Jaworek *et al* 2014, Pongrac *et al* 2014a, 2016, Borra 2018). It was also proved experimentally that the glow corona discharge does not destabilize the electrospraying mode unless the streamer discharge regime occurs. It was proved by photographic method with long exposures and by spectroscopic measurements that the glow corona discharge is normally present during electrospraying for sufficiently conducting liquids (Macky 1931, Schultze 1961, Giao and Jordan 1968, Hoburg and Melcher 1975, Bailey and Borzabadi 1978, Ballinger *et al* 1978, Ogata *et al* 1978, Hara and Akazaki 1981, Meesters *et al* 1992, Cloupeau 1994, Jaworek and Krupa 1997, Jaworek *et al* 2005, 2014, Stommel *et al* 2006, Bruggeman *et al* 2007, Pongrac and Machala 2011, Shirai *et al* 2011b, 2012, 2014, Elsawah *et al* 2012, 2013, Machala *et al* 2013, Kim *et al* 2014, Pongrac *et al* 2014a, 2014b, 2016, Kovalova *et al* 2016).

This paper reviews the state of knowledge regarding the physical processes and phenomena occurring in low temperature plasmas generated by electrical discharges during electrospraying of liquids, and the effect of such plasmas on the

J. Phys. D: Appl. Phys. **52** (2019) 233001

Topical Review
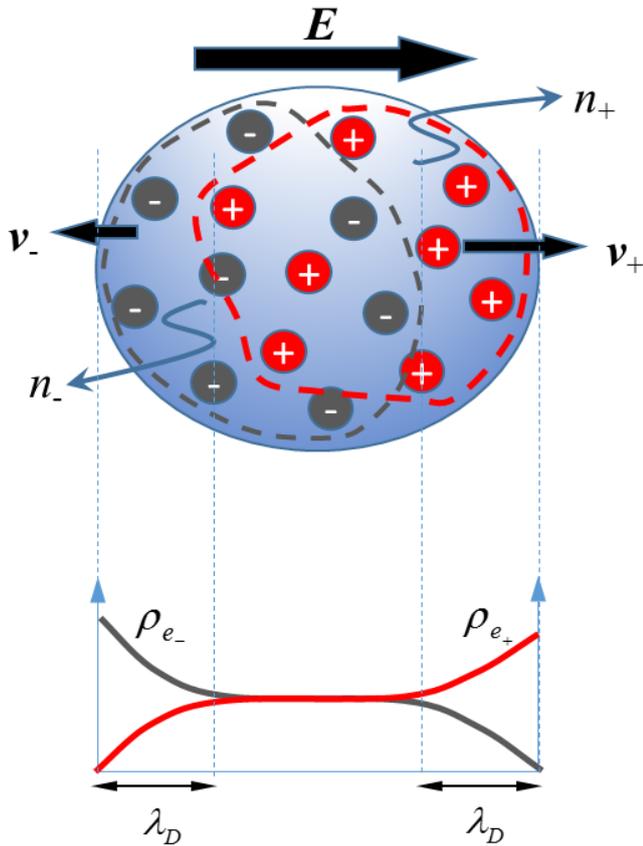
Figure 1. Basic mechanism of charge migration and charge layer formation in a liquid with free surfaces under an externally applied electric field E. λ_D would be the thickness of the layer of charges (Debye length) when a final equilibrium state is reached. v_+ and v_- are the relative velocities of positive and negative species, respectively, where n_+ and n_- are their number concentration per unit volume. Reprinted from Gañán-Calvo *et al*, Copyright (2018), with permission from Elsevier.

Figure 2. Typical configuration of the apex of a steady Taylor cone-jet electrospray, with the corresponding characteristic quantities discussed in the text. Reprinted from Pantano *et al*, Copyright (1994), with permission from Elsevier.

electrospraying process. The plasma in a glow corona discharge mode can play a stabilizing role in the stable cone-jet mode of spraying generation, but streamer discharges disturb the electrospraying process. Although this phenomenon can be undesired for certain applications of electrospraying, it was also utilized for the decontamination and sterilization of electrosprayed liquids by the generation of discharges of higher energy (streamer, spark) (Machala *et al* 2010, 2013, Kovalova 2013, 2016).

2. Electrospray principles and mechanisms

Basically, when a liquid carrying a volume charge density ρ_e (i.e. an electrolyte or low conductivity liquid) is subject to an electric field with intensity E, it causes an electrohydrodynamic reaction where an equivalent pressure gradient ∇P_e comparable to $\rho_e E$ drives the charges along the applied field lines. However, unless the liquid is electrically non neutral these gradients point in opposite directions (figure 1) for each ionic positive and negative species, moving the charges of corresponding polarity in their appropriate direction (the formal expression of these bulk forces is the divergence of the resulting Maxwell stress tensor, Saville (1997)).

Eventually, this simple picture entails the accumulation of charges of the same polarity at the exposed surface of the liquid, which form a dense charge layer with a high charge density σ_e and thickness—the Debye's length—such that the thermal and electroosmotic diffusion become balanced due to the high normal electric field E_n built on the outer side of the liquid surface. That outer side is normally a dielectric environment such as vacuum, air, or a dielectric liquid (e.g. oil). In these conditions, the surface charge shields the rest of inner bulk charges, and only a small potential gradient along the charged liquid surface may become noticeable in comparison with E_n, such that $\sigma_e \sim \varepsilon_o E_n$. This is the typical picture of *leaky dielectric liquids* under the action of large electric fields (Melcher and Taylor 1969). Eventually, the normal stress that accelerates the liquid from its surface, often known as the *electrostatic suction*, is of the order of $\tau_n \sim \sigma_e E_n \sim \varepsilon_o E_n^2$ (figure 2). Usually, modest tangential stresses $\tau_s \sim \varepsilon_o E_n E_s$ may also appear because of small variations of the potential along the length L on the surface, with $E_s \sim \Delta_s V / L$, as a consequence of local limitations in the process described of charge relaxation on the surface (Gañán-Calvo *et al* 2016).

On the other hand, surface tension—always present in free liquid surfaces—entails an equivalent normal stress $\tau_n = \sigma_l \nabla_s \cdot \mathbf{n}$, where ∇_s is the surface divergence, $\mathbf{n}$ is the unit normal to the surface, and σ_l is the surface tension of the liquid-environment interface. Moreover, the viscous stresses

$$\boldsymbol{\tau}_v \cdot \mathbf{n} = \mu_l \left(\nabla \mathbf{v} + \nabla^T \mathbf{v} \right) \cdot \mathbf{n} \qquad (1)$$

are also present at the surface, where μ_l is the viscosity of the liquid. Under the action of all these surface stresses, the liquid meniscus rapidly elongates in the direction of the applied potential difference, and eventually a liquid ejection takes place (Gañán-Calvo *et al* 2016). In most electrospray conditions, the electrostatic suction becomes comparable to the kinetic energy generated in the liquid ejection, i.e.

$$\varepsilon_o E_n^2 \sim \rho v^2. \tag{2}$$

Depending on the combination of all geometrical and operating parameters, boundary conditions, and physical properties of the liquid and its surrounding environment, that ejection may take very different forms, among which the so-called steady Taylor cone-jet (STCJ) is the preferable mode of operation of electrosprays.

2.1. Spray current scaling laws

Two main properties of electrospray droplets are important from the practical point of view and for the theoretical analysis: the size distribution of the droplets and the electric charge carried by these droplets. The size distribution of droplets for various spraying modes has been measured by various authors in many papers. However, the charge carried by individual electrospray droplets is much more difficult to assess (Gamero-Castaño 2010), in contrast with the total spray current, measured and determined theoretically.

Fernández de la Mora and Loscertales (1994) carried out the dimensional analysis of the emitted current in STCJ, considering all the parameters involved in electrospraying process, and analysed the best collapse of experimental results. The current emitted in the cone-jet mode of spraying was scaled as:

$$\frac{I}{\sigma_l \left(\frac{\varepsilon_o}{\rho_l}\right)^{1/2}} = f_I \left(\varepsilon_r, \left(\frac{Q\rho_l\kappa_l}{\sigma_l\varepsilon_o\varepsilon_r} \right)^{1/2}, \frac{\left(\frac{\sigma_l^2\rho_l\varepsilon_o\varepsilon_r}{\kappa_l} \right)^{1/3}}{\mu_l} \right) \tag{3}$$

where Q_l is the liquid flow rate, ε_0 is the permittivity of the free space, σ_l is the surface tension, and κ_l, μ_l and ρ_l are the bulk conductivity, viscosity and mass density of the liquid, respectively. They concluded from the results of measurements obtained for six polar liquids that the spray current is independent of the dimensionless liquid viscosity in the range of:

$$0.022 < \frac{\left(\frac{\sigma_l^2\rho_l\varepsilon_o\varepsilon_r}{\kappa_l} \right)^{1/3}}{\mu_l} < 0.25 \tag{4}$$

and the spray current, in this viscosity range, could be reduced to:

$$I = \alpha_I \left(\varepsilon_r \right) \left(\frac{Q\sigma_l\kappa_l}{\varepsilon_r} \right)^{1/2} \tag{5}$$

where α_I is a function of the liquid permittivity $\varepsilon_l = \varepsilon_0\varepsilon_r$, and ε_r is the relative permittivity of the liquid. To reach to this scaling and the one of the emitted liquid jet radius, Fernández de la Mora and Loscertales assumed that the current was fixed

by a limitation of charge relaxation at the cone-jet transition: they proposed that the charge relaxation halted at a region of the cone-jet transition with a size comparable to the jet diameter. Using their estimate of the normal electric field at that region from the balance of surface tension and normal electric stresses, one easily gets the scaling law (5) assuming that $\alpha_I(\varepsilon_r)$ can be a constant. According to the authors, this law was satisfactorily compared to experiments in the cone-jet mode by Tang and Gomez (1994) and by Chen and Pui (1997), who measured the spray current in electrospraying of eight liquids in CO_2 atmosphere.

However, the function α_I was not a constant: it ranged from about 7 to 18 depending on the values of ε_r (see figure 11 in Fernández de la Mora and Loscertales (1994)). The relatively limited account of experimental results did not allow Fernández de la Mora and Loscertales (1994) to assess a more accurate functional form of $\alpha_I(\varepsilon_r)$.

One year before the publication of Fernández de la Mora and Loscertales (1994) and based on the opposite hypothesis to that used by those authors, Gañán-Calvo *et al* (1993) proposed that the surface charge was nearly relaxed everywhere, i.e. that the free charges reach a quasi-equilibrium state at the cone, cone-jet transition, and the jet. From this approach, they proposed a simpler scaling

$$I = 2.47(Q\sigma_l\kappa_l)^{1/2}. \tag{6}$$

This result suggested that the functional form of Fernández de la Mora and Loscertales (1994) was actually $\alpha_I(\varepsilon_r) = 2.47\varepsilon_r^{1/2}$.

Owing to the publication of this result in a conference abstract (Gañán-Calvo *et al* 1993), it was somehow neglected, while the scaling proposed by Fernández de la Mora and Loscertales (1994) rapidly earned a high reputation due to its overall good fitting. The scaling law (6) had to wait until both Hartman *et al* (1999) and Gañán-Calvo (1999) simultaneously verified it experimentally, numerically and theoretically. A more rigorous account of the different scaling laws that can be found depending on the three parameters appearing in dimensional analysis was proposed in Gañán-Calvo (2004); in particular, scaling similar to (5) can be formally derived in the range of small liquid flow rates.

Here, we briefly outline the physical arguments leading to the scaling law (6). This scaling law assumes that there is a characteristic length L associated to the transition region of the jet with diameter d where the electric current I changes from a dominant electroosmotic (Ohmic conduction) to dominant surface charge convection mechanisms (Gañán-Calvo 1997). Thus, one should have

$$I \sim \kappa_l E_s d^2 \sim \varepsilon_o E_n v d, \tag{7}$$

where $v \sim Qd^{-2}$ from mass continuity (assuming that the jet is so thin that viscous stresses rapidly impose a nearly flat velocity profile). The additional assumption of charge relaxation demands $L \gg d$, in order to have tangential fields smaller than the normal fields at the surface everywhere (otherwise, steady stable cone-jet solutions may not exist, as discussed in Gañán-Calvo *et al* (2018) and Ponce-Torres *et al* (2018)). The corresponding electrostatic equilibrium at the conical side

of the meniscus imposes the order of magnitude of the tangential field at the thin jet, i.e. $E_s \sim \left(\frac{\sigma_l}{\varepsilon_o L}\right)^{1/2}$ (from Taylor's solution). The power $W \sim I\Delta V \sim IE_s L \sim \kappa_l \sigma_l d^2/\varepsilon_o$ injected by the electric field should be of the order of the generation of kinetic energy per unit time $\rho Q^3 d^{-4}$, which immediately demands for the jet diameter:

$$d \sim \left(\frac{\varepsilon_o \rho_l Q^3}{\sigma_l \kappa_l}\right)^{1/6}. \tag{8}$$

This scaling law has been amply verified by published literature (see a compilation of data from many authors in Gañán-Calvo and Montanero (2009)). Finally, from the balance of electrostatic suction and kinetic energy (2), jet diameter (8) and equation (7), one obtains $I \sim (Q\sigma_l\kappa_l)^{1/2}$. Again, this simple scaling law for the emitted current in STCJ has been extensively verified for the electrospray of most leaky dielectrics, as shown in the compilation of data in Gañán-Calvo *et al* (2018). Interestingly, the scaling of the velocity of the liquid in the jet is a property of the liquid, independent of the liquid flow rate (Gañán-Calvo 1999):

$$v \sim \left(\frac{\sigma_l \varepsilon_o}{\rho_l \kappa_l}\right)^{1/3}. \tag{9}$$

One may observe the conspicuous absence of the liquid polarity in both scaling laws of the jet diameter and emitted current, which can make these scaling laws not fully applicable for high polarity liquids like water for the complete range of liquid flow rates where the STCJ is stable. These are cases more prone to exhibit electric discharges and low temperature plasma emissions.

The scaling laws presented above do not assume any polarity of the voltage at which the electrospray occurs and should be equally well applied to both positive and negative voltages. However, the stable Taylor cone-jet mode was not obtained for negative polarity in air environment when a high liquid conductivity is used, due to the large normal electric fields appearing in the cone-jet transition region and the jet (see for example, Kim *et al* (2014)) and the different ejection potential of cations and anions presented in the liquid. In principle, electrons are significantly more prone to ejection than cations present in the liquid, which may favour or trigger the formation of unsteady streamers and prevent the formation of stable Taylor cones under negative polarity for liquids of sufficiently high conductivity and large surface tension. However, under the conditions where gas ionization and low temperature plasma is established and stabilized, they stabilize the cone-jet by decreasing the effective electric field on the liquid surface. In these cases, hydration decreases the mobility of anions present in water, preventing the formation of stable coronas. In general, the compilations of experimental results presented in the relevant references (see for example Gañán-Calvo *et al* (2018)) correspond to electrospray at positive polarity, although many of the low conductivity liquids in Gañán-Calvo *et al* (1997) were electrosprayed at both positive and negative polarities without any appreciable differences,
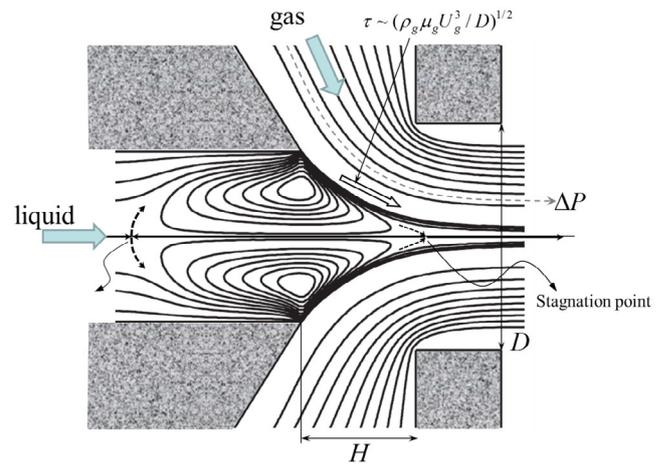
Figure 3. Typical flow focusing configuration. Reprinted figure with permission from Gañán-Calvo and Montanero, Copyright (2009) by the American Physical Society.

consistently with the absence of ion emissions expected in those cases.

2.2. Electro-flow focusing

The typical cone-jet structure is not a prerogative of the Taylor cone-jet. One may found similar tapering structures in many situations where any kind of concentrated suction effect may result in *tip streaming* (Basaran 2002, Eggers and Villermaux 2008). One of such structures appears in the so-called *flow focusing* (FF) mechanism (figure 3; Gañán-Calvo (1998), Anna *et al* (2003) and Garstecki *et al* (2005)), where two or more streams of immiscible fluids are discharged coaxially through an orifice or converging outlet (Deponte *et al* 2008).

When the outermost fluid stream is a gas and the inner stream is a liquid, which is fed from a capillary tube aligned with the outlet, one can observe a steady cone-jet structure that resembles the STCJ. In FF, the suction effect (Eggers 1998) is caused by the pressure drop ΔP_{FF} through the outlet, such that $\Delta P_{FF} \cong \rho v^2/2$. In STCJ, one may express the equivalent pressure drop ΔP_E driving the liquid ejection as

$$\Delta P_E \sim \rho_l v^2 \sim \left(\frac{\sigma_l^2 \kappa_l^2 \rho_l}{\varepsilon_o^2}\right)^{1/3}. \tag{10}$$

This equivalent pressure, which is driven by the applied electric field, is naturally independent of the liquid flow rate. The physics behind this result is the conversion of potential energy into kinetic energy: in both cases (electrospray and Flow Focusing) the potential energy available per unit volume is independent of the flow rate. This explains the intriguing dependence of v and ΔP_E on the properties of the liquid only. In a second-order analysis where both applied voltage and flow rate are considered, one may find a slight dependence on these parameters, but this is due to the finite ratio of feeding capillary to jet diameters. Indeed, the existence of the STCJ is linked to a relatively narrow range of applied potential differences between the liquid feeding source (normally, a capillary tube) and an electrode which may sustain a steady conical shape (Pantano *et al* 1994).

J. Phys. D: Appl. Phys. **52** (2019) 233001

Topical Review
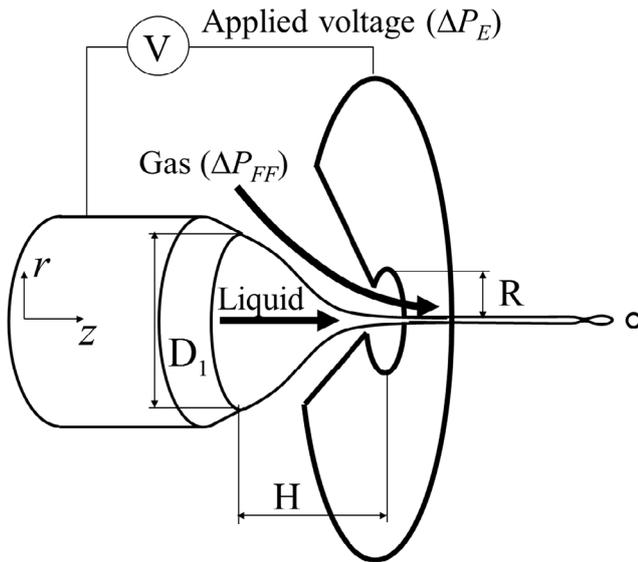
Figure 4. Electro-flow focusing configuration.

Thus, it is natural to think of a combination of both ΔP_E and ΔP_{FF} to produce augmented effects of enhanced stability, increased speed of ejection, and thinner jets. This combination is known as *electro-flow focusing* (EFF) (Gañán-Calvo *et al* (2006) and Gañán-Calvo (2007), figure 4).

One may introduce a non-dimensional parameter measuring the expected mechanical efficacy of the combination of mechanical and electrical forces as:

$$G = \left(\frac{\sigma_l^2 \kappa_l^2 \rho_l}{\varepsilon_o^2 \Delta P_{FF}} \right)^{1/3}. \tag{11}$$

When $G \ll 1$ one should expect a negligible influence of the electric field, while for $G \gg 1$ (normally occurring for relatively large liquid conductivities), the mechanical effect of the coaxial gas is negligible in the ejection—although it may contribute to the global stability of the cone-jet. The cases where G is of the order of unity yield enhanced results over both FF and STCJ for a given liquid. Moreover, the coaxial gas stream may be used as a means to control the electric discharges from the regions with larger surface electric field. This has made EFF attractive in mass spectrometry and surface desorption analytical techniques (Forbes and Sisco 2014, 2018).

3. Electrospray-corona studies

The electrical discharges occurring during electrospraying were initially studied by Zeleny (1920), Macky (1931), English (1948) and Schultze (1961). The research in this subject was intensified in 1970s because of the application of electrospray to mass spectrometry (Dole *et al* 1968). Electrospray as an ionization method for mass spectrometry of biomolecules (Fenn *et al* 1989) was among the soft ionization methods awarded by Nobel prize in chemistry in 2002 (John B Fenn and Koichi Tanaka). The investigations were focused on the of current–voltage characteristics of the electrospray, current

waveforms generated by the discharge and the spray droplets, the morphology of spray plumes and discharge types recovered from the photographic recordings. Later, more advanced physical tools were applied for the detection of generated species by mass spectrometry, light intensity measurements, and the detection of emission spectra by optical emission spectroscopy.

One of the first papers, which tackled quantitatively the problem of electric discharges in the electrospray was published by Burayev and Vereshchagin (1971). The authors considered the interaction of corona discharge with electrospraying for liquids with sufficiently high conductivity. The liquid drop at the capillary tip was approximated by semiellipsoid of revolution, for which the electric field was determined. The theoretical approach resulted in that the surface tension was the main parameter determining whether a liquid can be electrosprayed. The authors included the corona onset voltage to their considerations, and found the following two conditions for the transition from the dripping (or microdripping) mode to the cone-jet mode:

1. The bulk force on the liquid meniscus at the capillary outlet necessary for the initiation of electrospray has to be larger than that resulting from the surface tension force:

$$F_{ez} + F_g \geqslant F_\sigma. \tag{12}$$

2. The local pressure at the tip of liquid meniscus (cone apex), caused by the local electric field and gravity necessary for the formation of a liquid jet has to be larger than the surface tension pressure at the same point:

$$p_e + p_g \geqslant p_\sigma \tag{13}$$

where F_{ez}, F_g, and F_σ are the electric, gravitational and surface tension forces in the z-axis (nozzle axis) direction, respectively, and p_e, p_g, and p_σ are the electrostatic, hydrostatic, and surface tension (i.e. capillary) pressures at the meniscus tip, respectively.

The authors have shown that the mode of electrospraying depends on which of these inequalities is fulfilled first, with the voltage increasing. If the force-balance condition (12) is fulfilled first, the dripping or microdripping mode occurs. If the pressure condition (13) is fulfilled, the instability at the tip point of the meniscus leads to a thin jet formation from the cone apex, and the cone-jet mode is generated. However, if the voltage necessary to fulfill the condition (13) is larger than the ionization potential of the air (or in other gas, in which electrospraying takes place), the space charge of gaseous ions provided by the corona discharge will reduce the electric field at the cone apex, and the generation of the cone-jet mode will be prevented. This phenomenon can occur for liquids of high surface tension (like water in air), for which the electrostatic pressure p_e has to be higher than p_σ. Further increase in the potential of the nozzle can generate streamer discharge, which distorts meniscus and disturbs the jet stability, without generating the cone-jet mode. However, because of language barriers, this paper has been overlooked by the electrospray community.
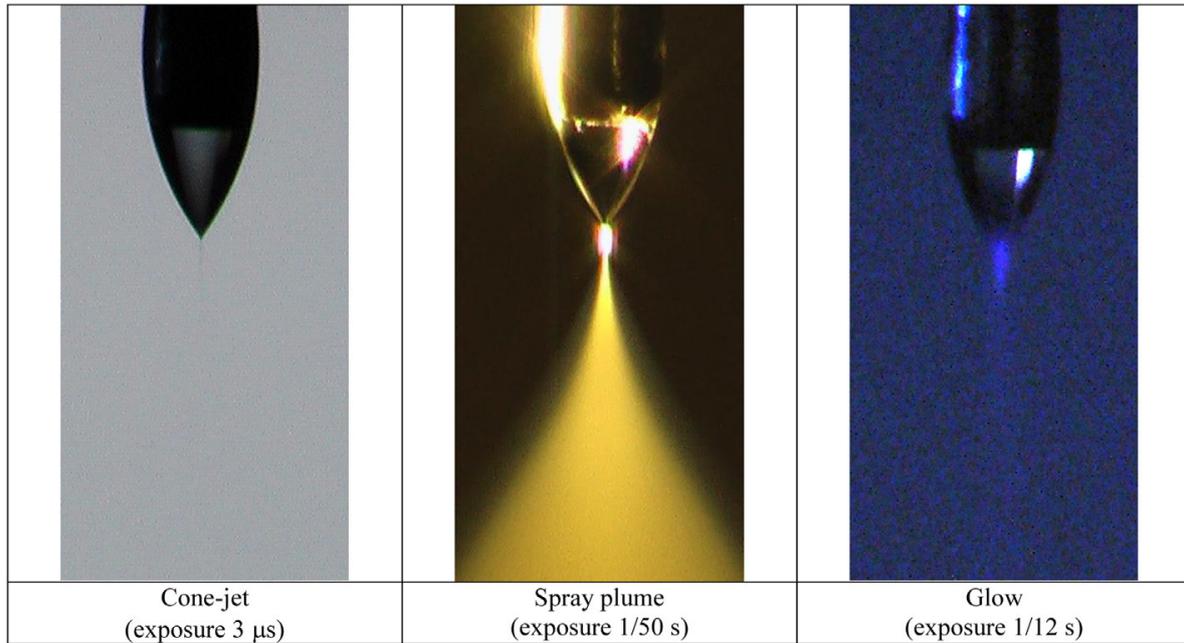
Figure 5. Cone-jet mode of electrospraying of water with faint glow corona discharge (0.12 ml h^{-1}, 12 kV, 5.7 μA). Reprinted from Jaworek *et al*, Copyright (2014), with permission from Elsevier.

For a liquid jet, Shorey and Michelson (1970) have approximated the tip of a jet by a hyperboloid of revolution and determined the electric field at the tip of the jet:

$$E = \frac{2U_c}{R_c \ln \frac{4h}{R_c}} \quad (14)$$

where U_c is the voltage applied to the capillary, R_c is the capillary radius, and h is the distance between the jet tip and the plate.

Smith (1986) has determined the electric field necessary for electrospraying in the cone-jet mode to be:

$$E_0 = \left(\frac{2\sigma_l \cos 49°}{\varepsilon_0 R_c} \right)^{1/2} \quad (15)$$

where σ_l is the surface tension of the liquid, and ε_0 is the permittivity of the free space.

Pantano *et al* (1994) resolved numerically the complete problem of the electrostatic shape of electrified liquid menisci attached to a capillary tube in the limit of zero emissions (liquid or charges), for a range of ratios of tube-electrode distance to tube diameter. To this end, they assumed that the asymptotic shape of the meniscus close to the tip of the meniscus was given by Taylor's solution. Under these conditions, the applied voltage and the volume of the meniscus are linked by a law that captures what the experiments reflect: lower voltages imply larger volumes. However, those ideal solutions implied infinite values of the electric field at the conical apex of the meniscus.

Gañán-Calvo (1997, 1999) and Jaworek *et al* (2016) determined numerically the electric field distribution adjacent to the liquid cone and jet of geometry and dimensions recovered from the photographs of the electrospray in the cone-jet mode. Gañán-Calvo (1997) obtained a peak value of 2.2×10^7 V m^{-1} at the cone-jet transition for an octanol jet of 25 μm, close to

the conditions of ionization of surrounding air (positive polarity, Hartmann (1984)). Jaworek *et al* (2016) concluded that the magnitude of electric field at the jet surface was of the order of 10^8 V m^{-1} for a water jet with a diameter of 10 μm, an applied voltage of 10 kV (positive polarity), and the space charge of droplets neglected. Their result indicated that the electric field is sufficiently high for the generation of corona discharge in the surrounding gas (air). The electric field magnitude at the capillary nozzle tip increases for capillaries of smaller diameter. Stommel *et al* (2006) have found that nozzles of smaller diameter produce a thinner liquid cone leading to higher electric field at the liquid-cone surface that generates a continuous glow discharge at lower voltages. The current–voltage characteristics shifts towards lower voltages for capillaries of smaller diameter, for both negative and positive polarity, in consistency with Smith (1986) and subsequent studies, and what can be expected for the formation of stable Taylor cones from very small capillaries (an interesting extreme case with capillaries as small as a few tens of nanometers can be found in Yuill *et al* (2015)).

It was shown in various papers that different forms of 'corona discharge' can occur, depending on the voltage and electrodes distance, similarly to discharges generated from a metal point electrode. The discharges that disturb the electrospraying are prebreakdown streamers, intermittent streamers, sparks, arcs, or burst pulses. Glow corona discharge or onset streamers do not disturb the jet (figure 5). When the streamers are generated, before the cone-jet mode is formed, the cone meniscus is distorted, preventing the stable jet formation (Zeleny 1914, English 1948, Tang and Gomez 1995, Borra *et al* 2004, Kim *et al* 2011, 2014, Jaworek *et al* 2014, Pongrac *et al* 2014a). For conducting liquids, for example water, streamers are generated from the liquid jet, and a visible discharge occurs at the same or lower potential before the meniscus starts to break-up

J. Phys. D: Appl. Phys. **52** (2019) 233001

Topical Review

(English [1948](#), Wampler *et al* [1993](#), Jaworek and Krupa [1997](#), Jaworek *et al* [2014](#), Pongrac *et al* [2014a](#)). The onset streamers did not appear in the CO_2 atmosphere (Kim *et al* [2014](#)).

For dripping and microdripping modes, the electric field at the liquid surface is usually lower than the threshold field for gas ionization. When the electric field increases to the magnitude higher than that required for gas ionization, the following discharge types and electrospray modes have been distinguished by Borra *et al* ([2004](#)):

1. For pre-onset streamers, when the electric field at the liquid meniscus is lower than the field required for the cone-jet mode generation, the unstable electric-dripping mode (spindle or ramified-jet mode) occurs due to electric field magnitude variations. The size distribution of droplets is not monodisperse due to transient variations of the electric field at the liquid surface.
2. For a stable glow corona discharge, when the electric field at the liquid surface is higher than the minimum field magnitude required for the cone-jet mode generation, a stable electrospray is generated (glow corona discharge-stabilized cone-jet mode). The size distribution of droplets is nearly monodisperse (standard deviation <0.3) due to stabilizing effect of the glow corona discharge (figure [5](#)).
3. For pulsed discharge (pre-breakdown streamers), when the electric field at the liquid surface is higher than the maximum field required for the cone-jet mode generation, the unstable electric-dripping mode is established again. The size distribution of droplets is again not monodisperse.

Similar effects were reported in other papers. An electric discharge can destabilize the cone-jet mode that results in changes of the size distribution of generated droplets, from monodisperse to bimodal or polydisperse (Rosell-Llompart and Fernadez de la Mora [1994](#), Borra *et al* [1996](#), [1999](#), Ku and Kim [2002](#)). For example, Borra *et al* ([1996](#), [1999](#)) observed for ethylene glycol that the cone-jet mode changed to the ramified jet or spindle mode when the streamer discharge was established, and large droplets (50–200 μm) were generated then. The distortion of the jet was attributed to the variations of space charge density in the interelectrode space, which changed the distribution of electric charge on the liquid surface, and deformed the meniscus profile leading to kink instabilities of the jet (Hoburg and Melcher [1975](#), Bailey and Borzabadi [1978](#), Kuroda and Horiuchi [1984](#), Jaworek and Krupa [1996a](#), [1996b](#), Borra *et al* [1999](#), [2004](#), Cech and Enke [2001](#)). However, many authors observed that the spray mode can be stabilized by the electric field generated by the space charge of gaseous ions after the onset of electrical discharge near the liquid surface (Kuroda and Horiuchi [1984](#), Borra *et al* [2004](#), Jaworek *et al* [2014](#), Pongrac *et al* [2014a](#)).

The discrepancy in those interpretations results from the differences in the type of discharge for both of those cases. It can be supposed that in the case the liquid jet is stabilized, the authors observed only the glow corona discharge, while other forms of gaseous discharges could only destabilize the electrospraying. When the glow corona is generated, an increase in supply voltage may not cause jet instabilities, but only causes

an increase in discharge current and discharge brightness, until the voltage magnitude at which the breakdown occurs (Zeleny [1914](#), Phan-Cong *et al* [1974](#), Bailey and Borzabadi [1978](#), Ogata *et al* [1978](#), Barber and Swift [1982](#), Meesters *et al* [1992](#), Cloupeau and Prunet-Foch [1994](#), Tang and Gomez [1995](#), Borra *et al* [1996](#), [1999](#), [2004](#), Jaworek and Krupa [1997](#), Ku and Kim [2002](#), Stommel *et al* [2006](#), Korkut *et al* [2008](#), Jung *et al* [2009](#), Kim *et al* [2011](#), Jaworek *et al* [2014](#), Pongrac *et al* [2014a](#)). The stabilizing effect occurs because an increase in the electric field reduces the tip radius of the cone meniscus and the diameter of the jet. When the radius of a meniscus is of one micron or smaller, the electric field is higher than the critical electric field for gas ionisation that promotes the glow corona discharge (Smith [1986](#), Joffre and Cloupeau [1986](#)). The stabilizing effect of the glow corona discharge has been confirmed by Ku and Kim ([2003](#)), which carried out experiments in air at a reduced pressure (~1 Torr). At such gas pressure, the glow corona discharge was generated easier, and the stabilizing effect of the discharge on electrospraying in the cone-jet mode, was demonstrated successfully.

Streamer discharges during electrospraying were observed only at higher voltages. The current–voltage characteristics of the electrospraying system for both polarities coincided only at lower voltages, for which the mechanisms of droplet generation and ionisation processes are similar. For higher voltages, these characteristics became different because the current pulses of streamers started to predominate over the spray pulses, and the total current at positive polarity was lower than the for negative one, at the same voltage magnitudes (Jaworek and Krupa [1997](#)).

It should be mentioned that in the case of electrospraying, only glow and (probably) onset streamer discharges are dependent on the geometry of liquid meniscus and the jet. Other discharges, particularly breakdown streamers, can develop directly from the capillary nozzle, regardless of the existing jet (Jaworek and Krupa [1997](#)). Hayati *et al* ([1987a](#)) observed that the location of the discharge depends on the conductivity of the liquid. For highly conducting liquids (water, glycerol), the discharge occurs at the apex of meniscus, but for liquids of low conductivity the glowing zone is confined only to the capillary rim.

The differences in the current pulses were attributed to the water molecules in the ambient air. Water vapours cause hydration of negative ions, decreasing their mobility (English [1948](#)). Giao and Jordan ([1968](#)) observed Trichel pulses at negative polarity, appearing irregularly with the frequency of a few kHz. They concluded that the repetition rate of Trichel pulses is influenced by the secondary emission from the electrode surface. The irregularity in the generation of pulses from water surface is probably because of water surface is a very poor secondary emitter. The frequency of Trichel current pulses measured by Pongrac *et al* ([2016](#)) for various electrolytes ranged from 70 kHz to 285 kHz with the voltage increasing from −5 kV to −9 kV (by electrode distance 10 mm). The authors also found that the corona discharge and space charge of H^+, Cl^-, Li^+ or OH^- ions is more important in determining the different shapes and propagations of the water jets for positive and negative polarities than the differences in mobility
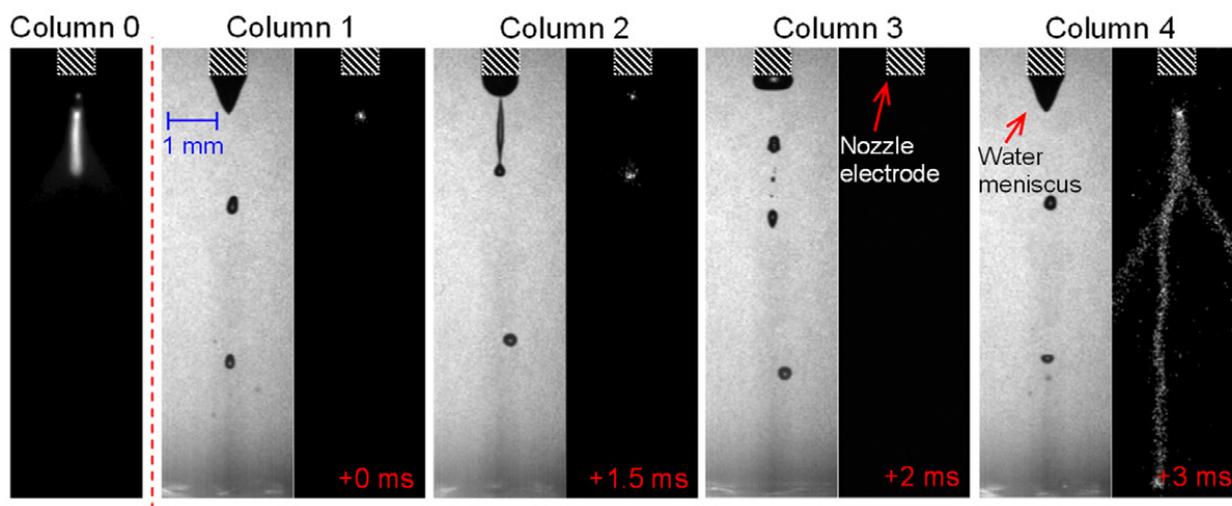
Figure 6. iCCD time sequence images of electrospraying of water in spindle mode (illuminated, columns 1–4 with exposure time 10 μs) with corona discharge (dark, columns 1–4 with exposure time 100 μs) for water conductivity 500 μS cm^{-1}, +6 kV, gap 1 cm, nozzle 0.8 mm o.d. and 0.6 mm i.d. iCCD dark image in column 0 with exposure time 5 s represents an integrated emission over the long period with many droplet formation cycles. Reproduced from Pongrac *et al* (2014a). © IOP Publishing Ltd. All rights reserved.

of cations and anions of the solutions (Pongrac *et al* 2016), which supports the importance of the potentials of ion emission in the establishment of stable coronas.

Pongrac *et al* (2014a) discovered that the dripping, spindle, and oscillating-spindle modes were generated synchronously with the streamer current pulses. Comparing the frequencies of current pulses recorded by an oscilloscope and frequency of droplets generation, retrieved from images obtained by high-speed camera, the authors concluded that the recorded current pulses correlate with the discharge pulses from the capillary nozzle (figure 6). From the recorded current pulses and emitted light pulses detected by a photomultiplier it was determined that each current pulse was delayed by about 4 ns after the emitted light pulse.

Bailey and Borzabadi (1978) observed that during electrospraying, the high-frequency current pulses generated by the discharge were superimposed on low-frequency pulses, which were probably generated by the droplets detaching from the capillary. When streamer pulses predominated over the spray pulses, the transition from dripping to microdripping or spindle modes was observed (English 1948). More intense corona (probably prebreakdown streamers or burst pulses) occurring during the cone-jet mode disturbed the spraying mode, which changed to spindle or multispindle mode (Cloupeau and Prunet-Foch 1994).

The distortion of the liquid jet by electrical discharges diminishes for higher liquid flow rates, when the kinetic energy of the jet is very high. Then the jet is stable even at higher voltages. These phenomena were observed, for example, by Jaworek and Krupa (1997) (at voltages of 20–30 kV, electrode distance of 50 mm, flow rate 100–200 ml h^{-1}) and Borra *et al* (1999, 2004) (voltage 20–30 kV, electrode distance 40 mm, flow rate 35–200 ml h^{-1}). Due to a large interelectrode distance only the glow corona discharge was visible at the meniscus and jet surfaces, without transition of this discharge to the streamers at those voltages. However, the

classical Taylor cone had not been generated at these flow rates, and the droplets produced by these modes were larger (for example, 50 to 150 μm by Borra *et al* (2004), or 30–70 μm by Jaworek and Krupa (1997, 1999a, 1999b)). From those results Borra *et al* (1999, 2004) concluded that the diameter of droplets is independent of the nozzle diameter in this electrospray mode, but only on the electric field at the liquid surface, which depends on the radius of curvature of the meniscus and jet. Hoburg and Melcher (1975) noticed that the critical magnitude of electric field for corona onset only slightly decreased with increasing liquid flow rate, which is consistent with the finding that the normal electric field on the jet is nearly independent of the liquid flow rate (Gañán-Calvo 1999).

Regarding the voltage polarity, various observations of corona patterns and their luminosity conducted by different authors lead to different results. Similar to electric discharges from a metal electrode, the type of discharge during electrospraying depends on the polarity of sharp electrode (capillary in the case of electrospraying). It has been found by many authors (Straub and Voyksner 1993, Cloupeau and Prunet-Foch 1994) that electrospraying from a capillary nozzle at positive polarity is less disturbed by corona discharge than that at negative. English (1948) found that the magnitude of electrospray onset voltage was virtually the same for positive and negative polarity, and the differences were only in the corona onset voltage. Yamashita and Fenn (1984) found that the corona onset voltage for negative polarity of electrospray nozzle is lower than for positive one. These results were confirmed by the recent studies by Kim *et al* (2014). Additionally, those authors have shown that the corona onset voltage for negative polarity is the same in air and CO_2, while for positive polarity the corona onset voltage is slightly lower in CO_2 than in air. Some observations for water showed that the corona onset voltage is close to the cone-jet mode onset voltage (Wampler *et al* 1993, Jaworek *et al* 2014). The electrospraying

in the cone-jet mode for negative polarity is possible only in electronegative gases, for example, SF_6 (Wampler *et al* 1993).

The length of jet from the apex of the Taylor cone to the point of its breakdown is shorter for negative polarity than for positive one, but this difference decreases with increasing flow rate of the liquid (leading to larger jet diameters and smaller surface curvatures), and the lengths became nearly equal for the Weber number We = 20 (Ogata *et al* 1978). Schultze (1961), Hoburg and Melcher (1975), Jaworek and Krupa (1997), Ku and Kim (2002), Borra *et al* (2004) and Kim *et al* (2011, 2014) recorded the visible corona (glow) at almost entire surface of the meniscus and jet, downstream to the jet break-up point, and also at the tip of capillary nozzle. From the photographs presented by those authors, it was unambiguously found that the excitation/ionisation processes take place in the vicinity of the tip of capillary and along the liquid jet. Because of this, the discharge pattern is quite different for positive and negative polarities. In the work by Jaworek and Krupa (1997), the glow corona discharge was equally well observed and of similar luminosity for positive and negative polarity, despite earlier results by Ogata *et al* (1978), who have noticed that for positive polarity, the corona discharge was generated from the surface of liquid jet at the cone-jet transition region (i.e. where the largest normal electric field on the surface develops), while for negative polarity, the corona was concentrated in the break-up region, i.e. at the tip of the liquid jet (i.e. where larger surface curvature develops). This interesting fact reveals the importance of both the nature of the surface charge and the surface curvature in the generation of corona. For both polarities, the glowing zone developed upwards with the voltage increasing. The results of Ogata and co-workers were similar to those obtained by English (1948) who observed that the discharge for positive polarity is more luminous than that for negative one.

Photographs presented by Shirai *et al* (2012) for ethanol confirmed the results of Ogata *et al* (1978), i.e. it was shown that the glow covered only the narrowest part of the jet. The differences between the results presented by these authors and those in other publications can be explained by the differences in the magnitude of electric field. At lower voltages used in the experiments by Shirai and co-workers (5 kV of negative polarity, electrode distance 0.5–2 mm) and Ogata *et al* (12.5–17.5 kV by 80 mm), the electric field assumed sufficiently high magnitude to gas ionisation only at surfaces of high curvature. For polyvinyl alcohol (PVA) solution of higher viscosity (40 mPa × s), used by Shirai *et al*, the meniscus was hemispherical, and multijet mode was observed with the jets originating from the liquid surface nearly halfway between the capillary rim and meniscus apex (Shirai *et al* 2011b). The glow was observed around the jet, at a distance of about 1 mm from the meniscus surface. With the increasing voltage the discharge also approached the surface of meniscus.

It was observed that, at the same voltage magnitude, the electrospray current from water meniscus at the capillary nozzle was lower than the discharge current from the same dry capillary without water feed, independently of the polarity of the nozzle (Jaworek and Krupa 1997, Kim *et al* 2011). This effect can be caused by the space charge of droplets, which have lower mobility than gaseous ions, and reduce the electric field at the outlet of the capillary nozzle.

General conclusion from this brief review is that the effect of electric discharge on electrospraying cannot be considered without regarding the type of discharge. Stable glow can stabilize the electric field at the capillary nozzle due to the space charge uniformly distributed around the nozzle tip that favors stable cone-jet mode generation. When the voltage is sufficiently high, the streamers produced in the interelectrode space distort the electric field and charge distribution on the liquid surface, and irregular modes of electrospraying (spindle, multispindle, ramified jet etc) occur, which produce droplets of polydisperse size distribution. Larger droplets of high electric charge produced in these modes additionally introduce an asymmetry in the electric field that results in off-axis deformation of the liquid meniscus and generation of further droplets in various directions (Jaworek and Krupa 1999a, 1996a, 1996b).

4. Effect of liquid properties on corona discharge

Various types of discharges can be observed in electrospraying, similar to the discharge from a metal electrode: onset streamers, glow corona discharge, pre-breakdown streamers, breakdown streamers, spark discharge, and arc. Glow corona discharge and arc (if it occurs) are usually pulseless, while the current waveform of other discharges is built from a series of pulses. Macroscopically, a streamer from a metal electrode occurs as a bright filament bridging the interelectrode gap for a short time, usually shorter than 1 μs. Actually, each streamer is a highly ionised, small 'plasma ball', known as a streamer head, which propagates from the sharp electrode with high field with the initial velocity of about 5×10^5 m s^{-1}, which decreases to about 1×10^5 m s^{-1} close to the plate electrode (Ohkubo *et al* 2005, Kanazawa *et al* 2009). The peak current of such a streamer can be higher than 1 A, but the time averaged discharge current is usually lower than 1 mA. The frequency of streamers and the time-averaged discharge current are increasing with the voltage increasing. Electrically generated plasma by the glow corona discharge is rather faint, with low energy of ions and electrons, and the discharge current is typically smaller than 1 mA.

Two parameters of electrosprayed liquid are of primary importance for the process of electrospraying and corona discharge generation: surface tension and electrical conductivity. The effect of liquid conductivity results from the electrochemical processes within the liquid meniscus at the capillary nozzle outlet, which are similar to those during electrolysis. If the sprayed liquid molecules are dissociated (water, electrolyte), the cations and anions flow in opposite directions, to the meniscus surface and to the metal nozzle walls, depending on the polarity of voltage applied to the capillary nozzle. After polarization, the only current flowing through the meniscus is that one due to the electric charge removed from the meniscus and/or jet surface by the detaching droplets. When a liquid with non-dissociated molecules is electrosprayed, the process is more complex. For negative potential of the capillary

nozzle, the negative charge of droplets results from the attachment of electrons to molecules of high electron affinity. These molecules are flowing to the surface of liquid, producing strong repulsion force on the meniscus and/or the jet. For the positive potential of the nozzle, the positive charge on droplets is generated by the removal of negative charge from molecules via electrochemical processes forming negative ions, which flow to the metal walls of the nozzle. Positively charged droplets are therefore depleted of electrons (Bruins 1998) or are protonated (Skarja *et al* 1998, Sjöberg *et al* 2000, Cech and Enke 2001).

It has been noticed that not all negative ions are removed from the liquid to the metal walls at positive potential, but only about 25% or less. As a result, the charge-to-mass ratio of electrosprayed droplets for positive polarity is lower than for negative one. In general, with the liquid conductivity κ_l increasing, the jet diameter, its length, and the droplet size are smaller, which causes an increase in the specific charge (q/m ratio) of the spray (Smith 1986, Kebarle 2000).

The effect of voltage polarity on the critical voltage for microdroplets formation and on the size of droplets for conducting liquids has been explained by Poncelet *et al* (1999), for the case of sodium alginate solution. For negative polarity of the nozzle, the negative ions of alginate polyelectrolyte migrate from the solution to the meniscus and jet surface. The mobility of these ions is lower than the Na^+ ions and their migration to the surface takes much longer times. For a given electric potential and liquid flow rate, the surface density of the electric charge will be lower for the negatively charged needle, and, consequently, the surface tension will be higher that results in larger droplet size and higher critical potential (Fernandez de la Mora 2007). On the other hand, for positive polarity, the Na^+ ions of higher mobility build the surface charge on the meniscus surface faster, which decreases the surface tension and smaller droplets are generated at lower critical voltage.

Kim *et al* (2014) noticed that in air, the frequency of droplets generation in microdripping mode was higher for positive polarity than for negative, but in CO_2, this trend has been reversed, and the negative potential has generated droplets with higher frequency. The authors concluded that the voltage of transition from the dripping to microdripping mode is caused by the corona discharge.

The corona current in electrospraying depends mainly on the ionisation processes in the gas surrounding the liquid surface (Phan-Cong *et al* 1974, Jaworek and Krupa 1997, Gemci *et al* 2002). Hara *et al* (1979, 1980) reported that the amplitude of corona current pulses and their frequency decrease with increasing liquid conductivity. However, other studies did not find any correlation between liquid conductivity and intensity of specific emission lines generated during the discharge (Jaworek *et al* 2005). Pongrac *et al* (2014b) determined the frequency of prebreakdown streamers in electrospray, and concluded that the frequency decreased with increasing water conductivity. For example, the frequency was 5.6 kHz for liquid conductivity of 10 μS cm^{-1}, and it decreased to 0.65 kHz for 10 000 μS cm^{-1}. Current pulses for negative polarity, recorded by Hara *et al* (1979, 1980), consisted of successive

Trichel pulses of small amplitude that indicated the existence of faint streamer discharge. For positive polarity, the discharge was more complex: the first single pulse was followed by a steady current of corona (probably glow) discharge.

Pongrac *et al* (2014b) observed that the breakdown voltage for corona-to-spark transition decreased with increasing conductivity of the liquid. The authors also observed that the jet acceleration also depended on the liquid conductivity, and it was 4060 m s^{-2} for water of conductivity of 2 μS cm^{-1}, and decreased to 520 m s^{-2} for highly conducting liquid of 400 μS cm^{-1}, as shown in figure 7. The corona onset voltage decreased with increasing liquid conductivity (from 0.49 to 11.5 mS cm^{-1}). Similar effect was obtained by Shirai *et al* (2014).

It was shown that spray current and light intensity of corona discharge at the liquid surface in the cone-jet mode increase with liquid conductivity (Schultze 1961, Smith 1986, Hara and Akazaki 1981, Hayati *et al* 1987a, Straub and Voyksner 1993, Borra *et al* 1999, Sugimoto *et al* 2001, Dwivedi *et al* 2004, Shirai *et al* 2014, Pongrac *et al* 2014b), but at negative polarity, the liquid conductivity does not affect the current in the multijet mode for various liquids (water, methanol, ethanol, water-methanol mixture), until the voltage increases to the magnitude at which partial breakdown or the corona glow is generated (Yamashita and Fenn 1984). Borra *et al* (2004) reported that the operating range of stable cone-jet mode had shifted towards higher flow rates and higher voltages when the conductivity of water solution increased from 0.11 mS m^{-1} to 5 mS m^{-1}. This effect was caused by the stabilization of electrospraying mode by the glow corona discharge, whose onset voltage increased with liquid conductivity. However, for conductivity higher than 5 mS m^{-1}, the impulse discharges (probably streamers) developed from the nozzle and disturb the cone-jet mode. For liquids of low conductivity, the nozzle edges are more exposed to electric field that results in intense glow corona discharge mainly near the metal nozzle, but only faint glow was observed close the liquid surface (Hayati *et al* 1987a, Jaworek and Krupa 1997, Borra *et al* 1999).

Regarding the effect of surface tension on electrospraying, many authors claim that for liquids of low surface tension (acetone, ethanol), the Taylor cone is formed, and the cone-jet mode is generated for voltages lower than corona onset voltage (Borra *et al* 1996, 1999, Cole 2000). With increasing surface tension, the voltage required for a stable operation of electrospraying in the cone-jet mode also increases because higher electric field is needed to balance the surface tension force (Cech and Enke 2001). For liquids of higher surface tension (water, ethylene glycol) the generation of the cone-jet mode in air is limited by corona discharge, which onsets for a voltage lower than that required for electrospraying (i.e. the electric field magnitude needed to overcome the surface tension is higher than that initiating the corona discharge, and the corona is generated first) (Burayev and Vereshchagin 1971, Smith 1986, Ikonomou *et al* 1991, Fernandez de la Mora and Gomez 1993, Cloupeau and Prunet-Foch 1994, Borra *et al* 1996, 1999, Kebarle 2000, Cech and Enke 2001, Fernandez de la Mora 2007).
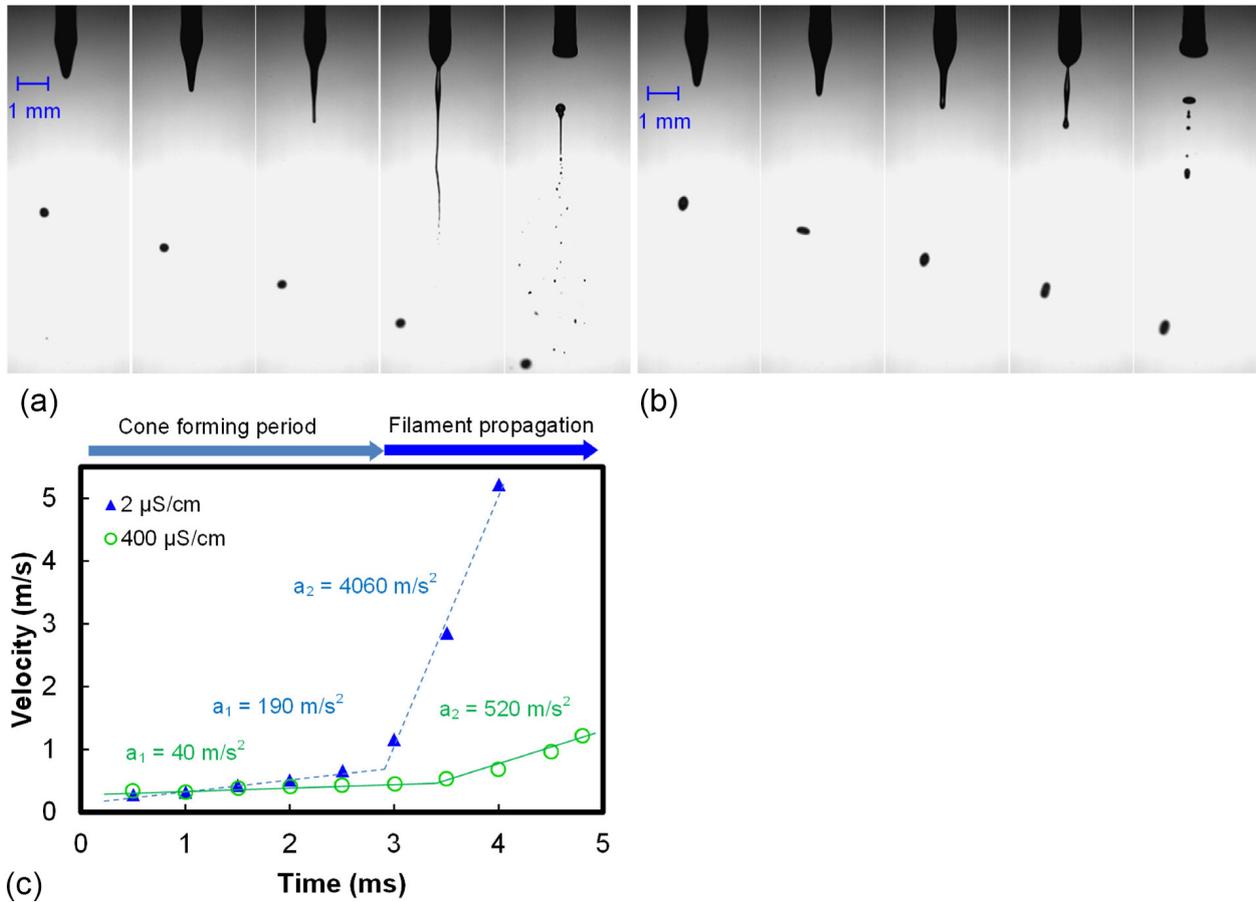
Figure 7. High-speed camera sequence of the spindle mode electrospray with water of (a) low conductivity 2 μS cm^{-1} and (b) high conductivity 400 μS cm^{-1} (10 000 fps, 1 μs gate time, time interval 700 μs, flow rate 0.4 ml min^{-1}, voltage +11 kV, 5 cm gap). (c) Comparison of water filament velocities during the cone formation and filament propagation for 2 different conductivities. Reprinted by permission from Springer: Nature Eur. Phys. Pongrac *et al* (2014b).

5. Spray current versus discharge current

The electric current carried by monodisperse droplets charged to a half of the Rayleigh limit is:

$$ I = 6Q_l \sqrt{\frac{2\sigma_l \varepsilon_0}{D_d^3}} \qquad (16) $$

where Q_l is the liquid flow rate, ε_0 is the permittivity of the free space, σ_l is the surface tension of the liquid, and D_d is the droplet diameter. Unfortunately, the scaling laws reviewed in section 2 do not take into consideration the current carried by the gaseous ions.

The problem of distinguishing between the charge carried by electrospray droplets (*electrospray current*) and that conducted by gaseous ions due to corona discharge (*discharge current*) becomes important when the total current is used for the estimation of the mean size and charge of droplets. These estimates can be determined from the ratio of liquid flow rate and the total current measured at the spray collector assuming a droplet charge hypothesis like the one leading to equation (16). In fact, a measurement of a single variable (total current in this case, independently of whether corona is present or not) cannot resolve simultaneously two unknowns (size and charge) unless one makes a hypothesis linking those

unknowns. This is why the assumption (16) is usually used while estimating the size. However, because of ionic current owing to the corona discharge, this method overestimates the droplets' charge and underestimates the mean droplet size (Jaworek and Krupa 1997, 1999a, Borra *et al* 2004, Korkut *et al* 2008). For example, Ku and Kim (2002) studied the effect of electrical corona occurring during electrospraying on the electrospray droplets characteristics for highly viscous liquids (NaI doped glycerol, 560–1400 mPa × s). The authors had shown that the mean diameter of droplets measured by Aerosizer can be two to six times greater than that predicted by the scaling laws published in the literature, based on the total current estimations. One explanation could be the overestimation of the droplet charge due to electric discharges. Another is the effect of liquid viscosity which may increase significantly both the jet diameter and the jet breakup wavelength. Thus, one should use the scaling laws for high viscosity liquids to correctly ascertain the contribution of corona discharges in those cases. The scaling laws for high viscosity liquids have been discussed for example in Gañán-Calvo (2004) and Higuera (2010).

From the comparison of electrospray current with the discharge current from the same dry capillary nozzle without feeding the liquid, it was concluded that the charge carried by

J. Phys. D: Appl. Phys. **52** (2019) 233001

Topical Review
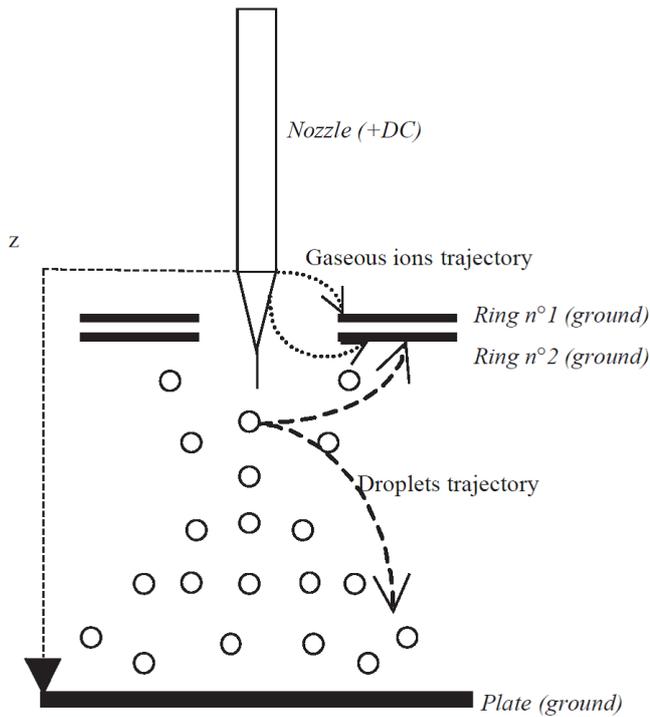
Figure 8. Schematic of the electrospray system comprising two grounded flat ring electrodes placed coaxially with the electrospray nozzle that separate the spray current and the discharge current. Reprinted from Borra *et al*, Copyright (2004), with permission from Elsevier.

gaseous ions can have a significant contribution to the total current measured at a collector (Jaworek and Krupa 1997). It was estimated from the measurement of the mean droplets' charge and the flow rate that the droplets carry only small amount of the total current.

In order to separate the spray current and the discharge current, Borra *et al* (2004) developed a measuring system comprising two grounded flat ring electrodes placed coaxially with the electrospray nozzle, a few millimetres beneath the tip of the nozzle, as depicted in figure 8. The upper ring collected gaseous ions, the lower ring gaseous ions and fine droplets, while the plate electrode beneath only the spray current.

Due to differences in the mobility of ions and droplets, the gaseous ions generated by electric discharge were collected on the first ring (glow corona discharge current), and the droplets were deposited onto the second ring, placed beneath the first one, and on the grounded plate beneath (electrospray current). From those experimental results, the authors determined the relation between the spray current and glow-corona current for the glow-stabilized cone-jet mode (Borra *et al* 2004, Borra 2018):

$$I_{spray} \propto Q_l^{0.2} I_{glow}^{0.1} \kappa_l^{0.2} \tag{17}$$

$$I_{total} = I_{spray} + I_{glow} \tag{18}$$

where κ_l is the liquid conductivity, Q_l is the liquid flow rate and I symbols are the currents. From these experiments, Borra *et al* (2004) have determined also the mean droplet diameter for the glow-stabilized cone-jet mode, which is dependent on the corona glow current:

$$d \propto Q_l^{0.5} I_{glow}^{-0.04} \kappa_l^{-0.2}. \tag{19}$$

The authors noticed that the operating range of stable cone-jet mode shifted towards higher flow rates and higher voltages when the conductivity of water solution increased from 0.11 mS m^{-1} to 5 mS m^{-1}. For conductivities higher than 5 mS m^{-1}, the glow changed to streamer discharge, and the glow-stabilized cone-jet mode disappeared. An important result of those investigations was that the spray current carried by the charged droplets can be much lower than the corona-discharge current. In the case of electrical discharges from a capillary nozzle, the ionic current can have a great contribution to the total current, and this result cannot be ignored in the research of electrospraying. Similar results for other spraying modes, not stabilized by glow corona discharge, particularly for the cone-jet mode, are not known yet.

Jaworek *et al* (2014) investigated current voltage characteristics of the electrospray system for distilled water (conductivity $0.97 \times 10^{-3} \text{ S m}^{-1}$), methanol ($0.165 \times 10^{-3} \text{ S m}^{-1}$), ethanol ($2.5 \times 10^{-4} \text{ S m}^{-1}$) and ethylene glycol ($2.25 \times 10^{-5} \text{ S m}^{-1}$), and for dry capillary nozzle for comparison, for three values of the flow rate (0.12 ml h^{-1}, 1 ml h^{-1}, and 10 ml h^{-1}). The current increased steadily with the voltage increasing from the corona onset voltage, similarly to the Townsend law (Townsend 1914), characterising corona discharge from sharp metal electrode:

$$I = \alpha U (U - U_0) \tag{20}$$

where U is the voltage between the electrodes and U_0 is the corona onset voltage. However, the spray current and discharge current have not been distinguished.

For all the liquids tested by Jaworek *et al* (2014), the total current only weakly depended on the liquid flow rate that can additionally suggest that the discharge current is the main component of total current, and confirmed the findings of Borra *et al* (2004) for water (see equation (17)). A significant departure of discharge current characteristics from the quadratic Townsend law was exhibited by methanol and ethanol only, for higher flow rates (10 ml h^{-1}). Regarding the close similarity between current–voltage characteristics of electrospray and for dry capillary presented in that paper (Jaworek *et al* 2014), two possible explanations can be suggested: (1) the main component of the total electrospray current is the gaseous ions current, (2) the contribution of droplets current and discharge current for those liquids changes with voltage. The first conclusion was suggested previously in the paper Jaworek and Krupa (1997) and was confirmed by the measurements by Borra *et al* (2004) (equation (17)) who separated the ionic and droplet currents. The second explanation, which seems to be more probable, is that the glow corona discharge is generated for lower voltages, and the current is mainly conducted by droplets in the dripping, microdripping and cone-jet modes (if present). For higher voltages, when burst pulses or streamer discharges are generated, the ionic current becomes dominant and the contribution of the charged droplets can be ignored. This explanation seems also to be consistent with the measurements carried out by Borra *et al* (2004) (figure 4

J. Phys. D: Appl. Phys. **52** (2019) 233001

Topical Review

therein). It was also observed that the discharge from dry capillary is more stable than that when a liquid jet is generated at the nozzle outlet.

Ballinger *et al* (1978) observed the electrospraying of water, ethanol and formic acid at a constant hydrostatic pressure, and different gases: air, Ar, He, N_2, O_2. The dispersion of liquids into small droplets occurred only in N_2, O_2, and in air. In noble gases (He and Ar), the glow corona bridged the interelectrode gap at voltages much lower than in other gases, and the liquid was not electrosprayed (no measurable flow of liquid). The electrode distance was 10 mm and capillary pyrex glass tube with Pt wire ion injector was used. In air of lower humidity, the stability of electrical discharge was improved.

Lastochkin and Chang (2005) electrosprayed droplets by AC high voltage of frequency >10 kHz. They observed visible corona close to the capillary and jet surfaces. With the addition of Ar or He to surrounding air, the corona became more intense and larger droplets were generated at lower voltages. By high frequency excitation, the drop ejection occurred at voltages an order of magnitudes lower (<2000 V) than those used for conventional electrospray supplied with DC voltage. The droplets were larger than by DC excitation and the cloud of produced aerosol was electrically neutral. The rate of droplets production was at least two orders of magnitude lower than the AC frequency. This phenomenon was attributed to a normal Maxwell force acting on the jet surface due to an undispersed plasma cloud in the close vicinity of the meniscus and to the volume charge polarization within the liquid. The high frequency AC excitation of meniscus was particularly suitable for the electrospraying of dielectric liquids, without a need of using an ion injector.

It can be concluded from this brief overview that the charge carried by gaseous ions can have a significant contribution to the total current of electrospray. The ion current can be comparable to or even higher than that of liquid droplets. The space charge formed by the droplets and ions reduces the electric field at the liquid jet, and stabilizes the corona discharge current.

6. Mass spectrometry studies

In order to explain the role of electrical discharges in electrospraying used for the ionization of molecules in mass spectrometry, many authors have analysed the mass-spectrometry signals for identification of gaseous ions produced by the discharge during electrospraying. The interest in this phenomenon was motivated by the possible spurious signals, which could be generated in mass-spectrometer detector by the gaseous ions originating from the gas discharge (Sjöberg *et al* 2000). An additional possible detrimental effect of a discharge is a fast degradation of a nozzle used for the analyte dispersion, and generation of spurious signals due to ablation of the capillary nozzle by gaseous ions obtained in the discharge (Smith and Wood 2003).

Another reason for the interest in electrospray corona discharge is the potential risk of damaging of biological or other fragile samples analysed by mass spectrometry due to

ion bombardment, UV radiation, or free radicals produced in the discharge plasma (Liu *et al* 2007). The degradation of electrosprayed material was studied first by Teer and Dole (1975), who deposited polystyrene latex microparticles on an aluminium foil by electrospraying. The electron microscope micrographs of these particles revealed that about 10% of the polystyrene beads was degraded, but only when higher voltage of negative polarity (-24 kV) was applied to the nozzle. It was probably caused by the bombardment of these particles by electrons and gaseous ions produced by the onset-streamer discharges in nitrogen. Electrospraying at positive voltage, up to $+20$ kV, or in SF_6 atmosphere eliminated this degradation, because the SF_6 gas quenched the discharge. In order to prevent the destabilization of electrospraying process and unwanted chemical reactions due to gas breakdown between the capillary nozzle and the ground electrode, Tang and Gomez (1994) used CO_2 atmosphere. Other authors (see, for example, Thundat *et al* (1992), Tang and Gomez (1994), Chen and Pui (1997), Ijsebaert *et al* (1999, 2001), Uematsu *et al* (2004), Pareta *et al* (2005) and Xu *et al* (2006)) claimed that the high voltage used for electrospraying of a suspension of fragile materials did not degrade the molecules or the degradation was negligible.

In the early stage of investigations of electrospray-corona products by mass spectrometry, the gaseous ions originating from the discharge have not been detected in the mass spectra. Such experiments have been carried out for the cone-jet mode by Yamashita and Fenn (1984) for water, methanol, ethanol and water-methanol mixture, and Rosell-Llompart and Fernández de la Mora (1994) for ethylene glycol, water and water-methanol mixtures in air and CO_2. However, in later studies, the following ions resulting from electrical discharge from capillary nozzle at negative polarity have been recorded: NO_2^- and NO_3^- ions for water-methanol mixture (water percentage higher than 10%—Asbury *et al* (2000) and Dwivedi *et al* (2004)), and O_2^-, HCO_2^-, CO_3^- and NO_2^- (Wampler *et al* 1993, Kebarle 2000).

However, in the presence of electronegative SF_6 gas, the relative intensity of O^-, O_2^-, and NO_2^- ions (resulting from the solvent and/or analyte dissociation) in the mass spectra was reduced, whereas the ions resulting from SF_6 decomposition, such as F^- and HF_2^-, H_3O^+ ions in water, and $CH_3OH_2^+$ ions in water-methanol mixture appeared, because of the transfer of proton to methanol, which has the higher proton affinity (Ikonomou *et al* 1991). SF_6 gas quenched the discharges causing a decrease in $CH_3OH_2^+$ ions concentration. The expected SF_6^- ions, formed due to the electron attachment to SF_6 molecule, were not observed in the mass spectra (Wampler *et al* 1993). Pongrac *et al* (2016) observed that the jet formation and evolution during electrospraying in electronegative gases was the same for the same voltage magnitude, regardless of the polarity of the voltage applied to the capillary nozzle.

From these investigations, it can be concluded that the electrospray corona discharge can cause ionisation of gaseous molecules, analytes and solvents in the gas phase, causing erratic signals in mass-spectrometry detectors (Yamashita and Fenn 1984, Ikonomou *et al* 1991, Wampler *et al* 1993, Steward 1999, Kebarle 2000, Cech and Enke 2001, Dwivedi

J. Phys. D: Appl. Phys. **52** (2019) 233001

Topical Review

et al 2004). On the other hand, the discharge-induced ionisation can be responsible for the production of protonated molecules of high proton affinity (Ikonomou *et al* 1991, Zhou and Cook 2000).

Recently, ambient ionization at atmospheric pressure for mass spectrometry or ion mobility spectrometry attracted the interest of many researchers in the field. Various ionization techniques have been described that allow a quick and easy-to-handle analysis of samples under ambient conditions without or with only minor sample preparation. Among those, plasma-based techniques, including the low-temperature plasma probe using corona or dielectric barrier discharge, require very little resources thereby providing great potential for implementation in stationary or mobile analytical devices (Franzke 2009, Sabo and Matejcik 2012, Sabo *et al* 2015, Kiontke *et al* 2018a, 2018b)

7. Optical emission spectroscopy studies

Optical emission spectroscopy was applied as another method for the detection of corona discharge during electrospraying, but there are only a few papers on this subject (Meesters *et al* 1991, Jaworek *et al* 2005, 2014, Shirai *et al* 2008, 2014, Kim *et al* 2014). Optical emission spectroscopy provides various plasma parameters, such as ionization and excitation states of gaseous molecules and volatilized elements. From these data the gas composition, electron number density and temperature, ion temperature, and atomic/molecular concentration of various species in the gas can be determined. The electron number density in plasma can be determined from the Stark broadening of the spectral lines of H_β or H_α (at 486 or 656 nm, respectively). Plasma temperatures (electron, vibrational and rotational for molecular gases) can be determined from the Boltzmann diagram, which uses relative emission of the same atoms (or molecules) at different spectral lines (or vibrational bands/rotational lines) for different stages of electronic (or molecular) excitation, assuming that the excited states distributions of gaseous atoms or molecules is given by the Boltzmann statistics (Sember 2002, Laux *et al* 2003, Fantz 2006, Machala 2007). With the knowledge of the value of electron number density and neutral number density, the degree of ionization can be determined (Xiao and Staack 2014).

Meesters *et al* (1991) was probably the first who applied optical emission spectroscopy for the detection of emission spectra of electrical discharge in electrospraying of di-octyl-phthalate and methanol. They found only an excitation and vibrational bands of N_2 molecules, identifying the N_2 second positive system, and the N_2 first negative system in the measured spectral range. The excited O–H or C–H bonds have not been found. From these measurements, the authors concluded that the liquid cone does not participate in the discharge process.

From spectroscopic studies of electrical discharges, which occurred during electrospraying of conducting liquids in air at atmospheric pressures, presented by Jaworek *et al* (2005), the authors concluded that all electrospraying modes, except the dripping, are accompanied by gas ionization. Glow corona

or onset-streamers discharges, which were localized near the entire liquid surface, did not disturb the spraying process. The stability of spraying mode was disturbed when the pre-breakdown streamers occurred. The spectroscopic analysis indicated that nitrogen lines are the most intense in the emission spectra, however, also weak spectral lines characteristic of the elements and compounds dissolved in electrosprayed liquid, which were ionized or excited in the discharge, were identified at other wavelengths of the emission spectrum.

Shirai *et al* (2008) have investigated the emission spectra from electrified meniscus of ethanol. For a short-pulse microdischarge of current pulse amplitude of 1000 A and pulse duration of about 0.5 μs, the atomic hydrogen line of H_α at 656.28 nm, and an ionic nitrogen line of NII at 500 nm, were observed. From spectroscopic measurements of discharges at low discharge currents, generated between a plate electrode above the liquid and the liquid Taylor cones occurring at the liquid surface, the authors concluded that mainly surrounding gas molecules and atoms emit the light. With increasing discharge current, the liquid vaporizes, and the emission of metal ions from salts dissolved in the electrolyte can be observed (Shirai *et al* 2012). The liquid could evaporate due to an increased temperature in the discharge region of high current density at the tip of Taylor cone. In another experiment, Shirai *et al* (2007) investigated an explosion of a single ethanol drop falling between two horizontal sharp electrodes, spaced at 0.1–0.9 mm. The authors have found hydrogen spectral line H_α at 656.28 nm as the effect of ethanol vaporisation and dissociation. Shirai *et al* (2014) also investigated the emission spectra of a discharge from a Taylor cone formed at a capillary nozzle facing upwards, maintained at high negative potential. Only the N_2 second positive system was found in the emission spectra in air. Other spectral lines (like Na due to the addition of NaCl in order to change water conductivity) were not recorded.

Jaworek *et al* (2014) have studied the emission spectra for four liquids electrosprayed in the cone-jet mode: distilled water (conductivity 0.97×10^{-3} S m^{-1}), methanol (0.165×10^{-3} S m^{-1}), ethanol (2.5×10^{-4} S m^{-1}) and ethylene glycol (2.25×10^{-5} S m^{-1}). The electrospraying process was investigated only for positive polarity of the voltage applied to the capillary nozzle, in air at atmospheric pressure and at ambient temperature, by relative humidity of about 40%. The measurements were carried out for three values of the flow rate: 0.12, 1.0 or 10 ml h^{-1}. The emission spectra were measured in the spectral range from 200 to 1100 nm. The difference between the discharge in electrospraying and other types of electrical discharges is that the former is very faint, not visible and can be only photographically recorded by long exposure times of at least a few seconds. Another difference results from that one of the 'electrodes' in electrospraying is a liquid (jet), not a metal, and secondary electron emission from liquids is much weaker and occurs only at higher potentials than from the metals (Gaisin and Son 2005, Machala *et al* 2008, Bruggeman and Leys 2009).

In the electrospray system used by the authors, the corona onset voltage was between 9 and 10 kV, and the emission spectra could be recorded in the same voltage range, independently

J. Phys. D: Appl. Phys. **52** (2019) 233001

Topical Review
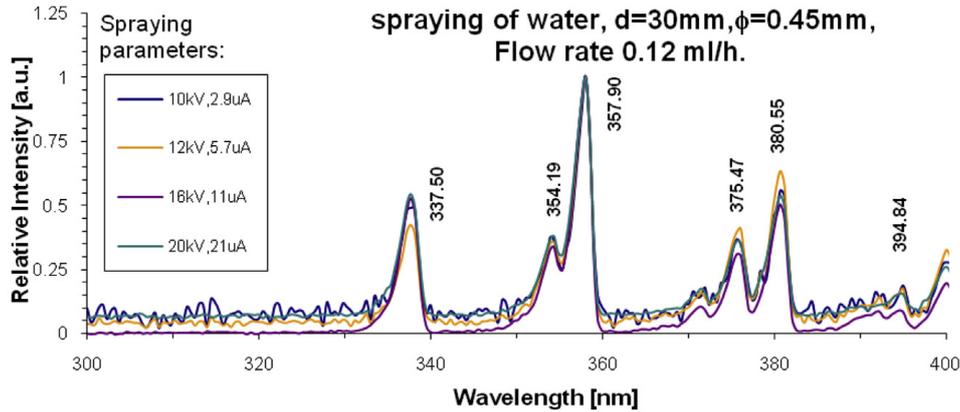
Figure 9. The emission spectra during electrospraying of water in air at atmospheric pressure for positive polarity of capillary nozzle, in the spectral range of 300–400 nm. Reprinted from Jaworek *et al*, Copyright (2014), with permission from Elsevier.

of electrosprayed liquid. Below 9–10 kV, the emission spectra have not been recorded. The emission spectra of the discharge near the jet were similar to those for dry capillary in air, for all the liquids tested, and were dominated by the second positive system (SPS) of nitrogen N_2 with the characteristic emission bands: 337.13, 357.69, 380.49, 375.54, 380.49, 394.30, 399.84 nm (Pearse and Gaydon 1963, Bruggeman *et al* 2010a, 2010b); figure 9.

Bands of the second negative system of N_2^+, which were observed in discharges in air from metal electrode at high discharge currents (see Czech *et al* (2011)), were not recorded in the case of electrospraying. Also, the band of OH-radicals ($A^2\Sigma \rightarrow X^2\Pi$, $(0-0)$) at 306.36 nm has not been recorded in those discharges. Possible products of decomposition or dissociation of molecules of other liquids in a discharge during the spraying of ethanol, methanol or ethylene glycol were also not recorded. The emission bands of NO_γ, usually observed at 237, 247 and 259 nm in corona discharge in air, were not recorded during electrospraying of liquids, probably because the energy of the discharge was too low. It can be concluded that the lack of OH radical spectral lines during electrospraying at lower voltages, before streamer discharge occurs, indicates that this discharge is not dangerous for fragile, in particular biological, samples. The authors noticed that the emission spectra are almost insensitive to the liquid flow rate (another evidence supporting that the potential energy driving the jet is independent of the flow rate), but the amplitude of specific peaks increases with increasing voltage within the range of stability of emission. The intensity of each peak varies in a large extent with the changes in the discharge type, but it is almost independent on the spraying mode.

The lines characteristic of O_2 (oxygen atomic line—777 nm), N_2 (nitrogen atomic line, 869.4 nm), and OH radicals (309 nm) appeared only for the streamer discharge. This result indicates that OH radicals can be produced only by the streamer discharge, as suggested by earlier results (see Sun *et al* (1997), Šunka *et al* (1999), Sugimoto *et al* (2001), Shmelev (2008), Shmelev *et al* (2009), Kanazawa *et al* (2009, 2011), Dilecce and De Benedictis (2011) and Elsawah *et al* (2012)), but are negligible for glow corona discharge. Kanazawa *et al* (2009) have generated positive streamer discharges over the

water surface. Besides the second positive system of molecular nitrogen, the authors recorded the emission of hydrogen atoms (H_α, 656.3 nm), OH radicals ($A^2\Sigma^+ - X^2\Pi$, 309 nm) and the atomic line of oxygen (O I, 777 nm). They discovered that the production of OH radicals takes place at the air discharge/water interface.

Jaworek *et al* (2014) have determined theoretically that the emission intensity of the spectral lines of corona discharge (glow, onset streamers) during electrospraying follows the third-degree polynomial function of the voltage at capillary nozzle:

$$\Phi = BU\left(U - U_0\right)\left(U - U_T\right) \tag{21}$$

where U_0 is the corona onset voltage, and U_T is the threshold voltage for the emission of a specific spectral line. The experimental results indicated that the threshold voltage U_T for the emission of most of the recorded spectral lines was in the same voltage interval of 9–10 kV as the corona onset voltage U_0. This relation was confirmed by spectroscopic measurements, and it holds until prebreakdown streamers occur (Jaworek *et al* 2014). This equation is valid for:

$$U > \max\left(U_T, U_0\right). \tag{22}$$

Kim *et al* (2014) also have used the optical emission spectroscopy to identify the spectral lines emitted by the corona discharge in air during electrospraying of water. The authors detected only the nitrogen second positive system and first negative band in the optical spectrum. The emission intensity of the discharge was higher for negative polarity of the discharge electrode than for positive. The emission by hydrogen (H_α line at 656.6 nm) was not detected, which indicates a negligible role of the discharge in water dissociation, due to low energy of this discharge. Also OH emission at ~306 nm was not detected, in agreement with Jaworek *et al* (2014). The lack of OH and H spectra confirmed by several authors, despite the interaction of the corona discharge with the sprayed water droplets, indicates that the H_2O molecule dissociation is too weak by the corona discharge and the emission spectra are dominated by N_2 SPS.

A similar result was reported by Machala *et al* (2007) who compared the emission spectra of streamer corona, transient

spark and (DC) glow discharge (cathode fall-driven glow discharge, not glow corona) with water cathode and found detectable OH emission only for the hot glow discharge with a high gas temperature (1900 K) inside the plasma channel, leading to strong water evaporation. In the streamer corona with the low gas temperature (350 K, measured from the N_2 SPS), the water evaporation and dissociation were too low to detect any OH spectra distinguishable from the overwhelming N_2 SPS spectra.

For pulse discharges, by an average current of 1–6 mA, Shmelev *et al* (2008, 2009) observed a glow discharge along a liquid jet of the length of 18 mm, the transition of this discharge to sliding surface discharge, and finally to low-current arc discharge by the current increasing to about 20 mA. The electron temperature in this discharge was estimated to be 1–2 eV, and neutral gas temperature, based on Planck distribution, to $T \approx 5000$ K. The light emitted by the discharge was generated by the excited/ionised gaseous molecules, water molecules, and products of water photolysis. The lines of excited atomic H^*, N^*, O^*, ions of N^+ and O^+, and lines of OH radical and other impurities have also been identified in the discharge.

In addition to the optical emission spectroscopy of the electrosprays interacting with corona discharge, electrospray in Ar atmosphere was used for generation of samples to the inductively coupled plasma spectroscopy (ICP-OES) (Brennan *et al* 2009).

Additional information on the role of electrical discharges in dissociation, ionization and excitation of water molecules was obtained from the investigations of various types of medium power discharges in water or at water surface. The '*medium power discharge*' in this paper refers to the discharges of 10–1000 W. In such discharges the time-averaged discharge current is of the order of magnitude of tens or hundreds of milliamps by a typical voltage of 10–20 kV. The discharges typically occurring in electrospraying, and studied in this paper, belong to the *low-power discharges* (<10 W), with a mean discharge current below 100 μA. Species like OH^*, H^*, O^*, $^1O_2$, O_2^-, O_3, H_2O_2, and HO_2 have been detected by optical emission spectroscopy in those discharges (Sun *et al* 1997, 1998, Šunka *et al* 1999, Kanazawa *et al* 2007, 2011, Bruggeman *et al* 2008b, 2009, 2010a, Bruggeman and Lyes 2009, Machala *et al* 2009, Dilecce and De Benedictis 2011, Elsawah *et al* 2012, Machala *et al* 2013, Kovalova *et al* 2016, Pyrgiotakis *et al* 2016, Hong *et al* 2018). The results show that hydroxyl radical (OH) is formed mainly within the discharge channel, and that the peak intensity of OH radicals is higher in spark discharge than in streamer discharge. The main transitions of OH radicals generated in a discharge are (Sun *et al* 1997):

$$A^2\Sigma^- (\nu' = 1) \rightarrow X^2\Pi (\nu'' = 0) \quad (282 \text{ nm})$$
$$A^2\Sigma^- (\nu' = 0) \rightarrow X^2\Pi (\nu'' = 0) \quad (309 \text{ nm}). \tag{23}$$
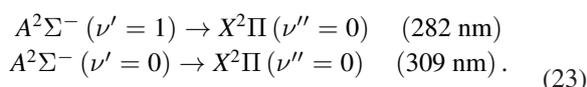
It was noticed that in streamer discharge only narrow peaks owing to OH radical are recorded while the spark discharge generates a continuous 'white' spectrum with the same characteristic peaks superimposed (Sun *et al* 1998). The

light intensity of OH radicals depends on the polarity of the streamer discharge and is stronger for positive discharge than for negative one (Sun *et al* 1997, 1998). For all time-averaged energies of the discharge, the concentration of hydrogen peroxide (H_2O_2) produced in the spark discharge was a few times higher than that produced by the streamer discharge due to a higher peak voltage and larger current density of the discharge, which promoted more intense excitation and ionization processes.

The conclusions from spectroscopic investigations presented by various authors can be summarized as follows:

(1) All electrospraying modes generated for conducting liquids in air or other gases at atmospheric pressures are accompanied by gas discharges. The glow corona or onset streamer discharges are localized near the liquid surface.
(2) The spectroscopic analysis indicated that nitrogen molecular bands are the most intense in the emission spectra (in air or nitrogen-containing gases) and can mask the emission of other compounds forming the electrosprayed liquid, especially OH radicals.
(3) Nevertheless, the spectral lines characteristic of the elements and molecules dissolved in electrospray liquids can also be detected at other wavelengths of the emission spectra.

8. Electrospray corona discharge prevention

In order to prevent the unwanted streamer or spark discharges, which destabilize the electrospraying process; several solutions have been proposed and tested in the literature (Borra 2018). These solutions can be divided into two groups. The first group comprises the methods that modify or stabilize the electric field in the vicinity of capillary nozzle, and the second, those that affect the surface tension of the liquid. To these methods belong:

1. Modification of the electric field in the interelectrode space by a ring or flat-plate electrode placed in the vicinity of the electrospray nozzle tip, co-axial with the nozzle, which is maintained at the same potential as that of the nozzle. The electrode allows controlling the divergence of electric field close to the liquid cone and jet to make it more uniform in order to sustain the glow corona discharge in wider voltage range (Meesters 1992, Borra *et al* 1996, 1999, 2004, Jaworek and Krupa 1996a, 1999b, Park *et al* 2004, Stommel *et al* 2006, Yurteri *et al* 2010). By this modification of electric field, the onset voltage of stable cone-jet mode shifts to lower magnitudes.
2. Reduction of electrospray nozzle diameter or sharpening its tip in order to increase the magnitude of local electric field and to reduce the length of ionisation zone around the liquid cone, which prevents the transition of glow corona discharge to streamer discharge of higher energy in the pulse (Lopez-Herrera *et al* 2004, Borra *et al* 2004, Stommel *et al* 2006). The nozzle of smaller diameter produces a finer liquid cone, leading to a higher electric

J. Phys. D: Appl. Phys. **52** (2019) 233001

Topical Review

field at the liquid surface that generates a continuous glow corona discharge stabilizing the electric field also for lower voltages. A similar effect can be obtained by decreasing the liquid flow rate, by which the jet diameter is reduced, and the electric field at the liquid interface increases, generating a stable glow corona discharge (Borra *et al* 1999).

3. Reduction of the conducting surface area of the nozzle exposed to the electric field by covering the tip of metal capillary with an insulating film (Stommel *et al* 2006), using an insulating capillary nozzle with an ion injector inside (Lopez-Herrera *et al* 2004, Kawamoto *et al* 2005, Park *et al* 2017), or using metal-coated insulating capillary (silica) with only the capillary tip uncovered (Kim and Lee 2004). By this way, the discharge current density is reduced that reduces the probability of streamer discharge development.

4. Self-controlling the potential at the capillary nozzle by applying a large resistance, of the order of magnitude of 10 MΩ to 10 GΩ, in series, which stabilize the discharge current (Jackson and Enke 1999, Amad *et al* 2000, Cech and Enke 2001, Jaworek *et al* 2005, 2014). When the current from the capillary nozzle increases due to unwanted pre-breakdown streamer development, the voltage drop over this resistance reduces the potential at the capillary tip and the discharge is quenched, preventing its transition to streamer, spark or arc discharge.

5. Increasing the dielectric strength of the surrounding gas, either by increasing the gas pressure or by using electronegative gases like O_2, SF_6, CO_2, or freon, which control the concentration of free electrons and prevent avalanche ionisation (Zeleny 1915, Burayev and Vereshchagin 1971, Yamashita and Fenn 1984, Hayati *et al* 1986, 1987a, Smith 1986, Cloupeau and Prunet-Foch 1990, 1994, Ikonomou *et al* 1991, Straub and Voyksner 1993, Wampler *et al* 1993, Rosell-Llompart and Fernandez de la Mora 1994, Tang and Gomez 1994, 1995, Chen and Pui 1997, Steward 1999, Sjöberg *et al* 2000, Lenggoro *et al* 2002, Yurteri *et al* 2010, Kim *et al* 2014, Pongrac *et al* 2016). A sheath gas (N_2), which removes ions from the nozzle surface was also used (Lenggoro and Okuyama 1997, Lenggoro *et al* 2000).

6. Reduction of the gas pressure (~1 Torr) that facilitates the generation of glow corona discharge in wider voltage range, without transition to the streamer discharge, and makes the electrospraying more stable than at atmospheric pressure (Ku and Kim 2003). In vacuum, the electric field is not modified by corona discharge, due to low ionic space charge, and liquids of very high surface tension, like for example, liquid metals, can also be electrosprayed in a stable cone-jet mode (liquid metal ion sources).

7. Reduction of the liquid surface tension via, for example, the addition of halogenated solvents or surfactants to the liquid, in order to promote generation of the cone-jet mode for lower voltages, before the streamer discharge can occur (Smith 1986, Borra *et al* 1999, Cech and Enke 2001).

8. Co-axial electrospraying (from two co-axial electrospray nozzles) by which a liquid sheath of lower surface tension (so-called driving liquid) is provided from the annular nozzle. The sheath liquid covers the core liquid of high surface tension (Loscertales *et al* 2002, Lopez-Herrera *et al* 2003, Barrero and Loscertales 2007). If the sheath liquid is unwanted for further processes, a liquid with high vapour pressure (easily evaporating) can be used for this purpose (Huber and Krajete 2000, Matz *et al* 2001).

9. Electrospray plasma applications

Recently, great attention has been paid to the investigation of plasma-liquid interactions, especially in atmospheric pressure plasma discharges over water or aqueous solution surfaces, as summarized by the latest large review and roadmap paper (Bruggeman *et al* 2016). This research is mainly motivated by new emerging applications of plasma discharges in biomedicine: starting from bio-decontamination and sterilization, through various medical therapies in dentistry, dermatology and cancer treatments, to applications in water cleaning, food production and agriculture (Laroussi *et al* 2012, Machala *et al* 2012, Fridman and Friedman 2013, Bruggeman *et al* 2016, Motyka *et al* 2017, Metelmann *et al* 2018). Since biological cells and tissues naturally live or are covered with aqueous solutions, the plasma interaction with cells and tissues is typically mediated through thin layers of water solutions. Furthermore, it was recently shown by many studies that so called '*plasma activated water*' (PAW), i.e. water or aqueous solutions or cell culture media that were treated (activated) by interacting with plasmas, can have many interesting applications in disinfection, wound healing, cancer therapies, as well as in seed germination and plant growth promotion without causing undesired side-effects or environmental burden (e.g. Lukes *et al* (2012), Puač *et al* (2017), Metelmann *et al* (2018) and Thirumdas *et al* (2018)). One of the most efficient ways of preparing the PAW is enhancing the transfer of plasma generated active species into water by increasing the surface to volume ratio, i.e. by reducing the water droplet sizes by aerosolation. Mechanical and ultrasonic ways of water atomization are typically applied, e.g. by Vaze *et al* (2017) in dielectric barrier discharge plasma aerosol charging and inactivation of aerosol-contained airborne bacteria, or Kordova *et al* (2018) who atomized the hydrogen peroxide/water solution through corona discharge and sprayed it onto plastic cups for microbial decontamination. Maguire *et al* (2015) combined mechanical aerosol nebulisation to control microdroplet transport through non-thermal radio-frequency discharge plasma with possible application to gas-phase microreactors and remote delivery of active species for plasma medicine. In a similar experimental concept, the same group introduced a new method of nanoparticle chemical synthesis based on liquid microdroplet irradiation with ultralow (<0.1 eV) energy of electrons from the non-thermal plasma (Maguire *et al* 2017).

Fundamental investigations of electro- and plasma-chemical processes due to electrical discharges used for organic contaminants neutralization, spores destruction or bacteria killing

at the air–water or other gas–liquid interfaces have been carried out by many authors (Sun *et al* 1997, 1998, Šunka *et al* 1999, Andre *et al* 2001, Mezei *et al* 2005, Sugama *et al* 2006, Baerdemaeker *et al* 2007, Liu *et al* 2007, 2008, Shmelev 2008, Shmelev *et al* 2009, Kanazawa *et al* 2009, Machala *et al* 2009, Locke and Shih 2011, Pongrac and Machala 2011, Shirai *et al* 2011a, 2011b, Pyrgiotakis *et al* 2012, Elsawah *et al* 2013, Kovalova *et al* 2013, 2016, Machala *et al* 2013, Kim *et al* 2014, Di Natale *et al* 2018, Hong *et al* 2018, Lamarche *et al* 2018). These processes were typically studied in low or medium power glow-corona, spark, streamer or arc discharges discharges. The electro-/plasma- chemical processes are based on the production of radicals in water or at its surface, ozone generation on the water–air interface, photochemical reactions due to ultraviolet radiation of the discharge, or shock waves produced by a pulsed discharge operating in the streamer or spark modes (Sun *et al* 1997, Šunka *et al* 1999, Sugimoto *et al* 2001, Shmelev 2008, Bruggeman *et al* 2008a, Machala *et al* 2009, Shmelev *et al* 2009, Kanazawa *et al* 2009, 2011, Bruggeman and Schram 2010, Dilecce and De Benedictis 2011, Elsawah *et al* 2012). Electrical discharges were also applied for trace contaminants detection in water by the spectroscopic measurement (Cserfalvi *et al* 1993, Kim *et al* 2000, Mezei *et al* 2001, Shirai *et al* 2011a).

In these publications, it was proved that OH radical was the most abounded product of medium-power electrical discharges with water. These radicals are produced by free electrons accelerated to energies sufficiently high to break chemical bonds of water molecule after collision (Sun *et al* 1998, Baerdemaeker 2007), for example, in the following reaction:

$$H_2O + e^- \rightarrow H^* + OH^* + e^-. \tag{24}$$

The reactive hydrogen peroxide can be synthesized in a discharge due to, for example, the following reactions (Sun *et al* 1998, Baerdemaeker 2007, Bruggeman and Schram 2010, Kanazawa *et al* 2011):

$$\begin{aligned} OH^* + OH^* &\rightarrow H_2O_2 \\ H^* + HO_2^* &\rightarrow H_2O_2 \\ H^+ + HO_2^- &\rightarrow H_2O_2. \end{aligned} \tag{25}$$
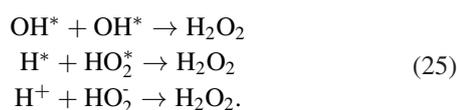
H_2O_2 diffuse outside the discharge channel, but strong UV radiation generated by spark discharge facilitates the photolytic decomposition of the molecule producing additional OH radicals (Sun *et al* 1998):

$$H_2O_2 + h\nu \rightarrow OH^* + OH^*. \tag{26}$$
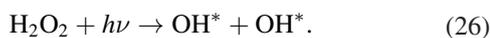
Because of this decomposition, a high concentration of OH radicals could be found in the discharge chamber. The electrohydrodynamic flow induced by the discharge causes that the concentration of OH radicals in a plasma reactor outside the discharge channel increases and becomes uniform (Kanazawa *et al* 2009, 2011). Besides free radicals production, hydrated protons ($H^+(H_2O)_{1-7}$) were also observed in the discharges at reduced pressures (Wróblewski *et al* 2001, 2003). Electrospraying was frequently used for the generation

of such protonated water clusters (Hulthe *et al* 1997, McQuinn *et al* 2007, 2009).

Water electrospraying seems very promising in combination with plasmas, since it allows integrating liquid atomization with electrical discharge into the same setup, using the same nozzle electrode, typically a hollow needle. So, on the contrary to preventing electrical discharges in electrospray due to their disruptive effects in some applications, here the electrospray combined with the streamer corona discharge are crucial to induce the desired decontamination of surfaces or water activation effects (Kovalova 2013, 2016). Hong *et al* (2018) also combined the underwater capillary discharge with electrospray for bacterial inactivation. With such discharge-electrospray setup, not only glow or streamer discharges can be combined with the electrospray, but also higher power spark discharges, as shown in figure 10. Strong hydrodynamic instabilities and pressure gradients in the spark discharge extremely perturb the stability of the electrospray modes; nevertheless, the PAW prepared by this way possesses very strong antibacterial effects (Machala *et al* 2010, 2013, 2018).

Electrospraying or aerosol charging in electrical discharges was also combined with plasma generated by dielectric barrier discharge (DBD) or other atmospheric pressure discharges (Borra 2006, Tatoulian *et al* 2006, Borra *et al* 2012). The technology called '*plasma-enhanced deposition process*' allows the production of highly stable polymer coating on other polymer substrate from an electrosprayed monomer. For example, this technology was used for the deposition of thin polymer film from electrosprayed di-ethyl-glycol monovinyl ether monomer as a liquid polymer precursor onto polyethylene substrate, which has been pre-treated with DBD at atmospheric pressure (Tatoulian *et al* 2006, Borra *et al* 2012). The DBD was used for the initiation of the reactive groups, which promoted the grafting polymerization of vinyl monomers and the interlocking between the deposited coating and the activated substrate. Non-thermal plasma discharges charge aerosol particles for electro-collection and trigger heterogeneous chemical reactions for organic and inorganic films deposition. Heat exchanges in thermal plasmas enable powder purification, shaping, melting for hard coatings and fine powders production by reactive evaporation (Borra 2006).

In summary, it should be noted that the electrospraying technology in combination with electrically generated plasma discharges seems very promising in applications to decontamination processes or to material processing. In this case, the liquid atomization can be integrated with electrically generated plasma within the same device by using the same power supply to the same capillary nozzle. Although some of the experiments discussed in this section were carried out for different electrode configurations and for discharges of higher energy than those typically met in electrospraying, and those results cannot be directly transferred to the discharges occurring in electrospray, the investigations can be very instructive for better understanding the chemical and physical processes, which could be expected during the electrospraying application to water decontamination.

J. Phys. D: Appl. Phys. **52** (2019) 233001

Topical Review
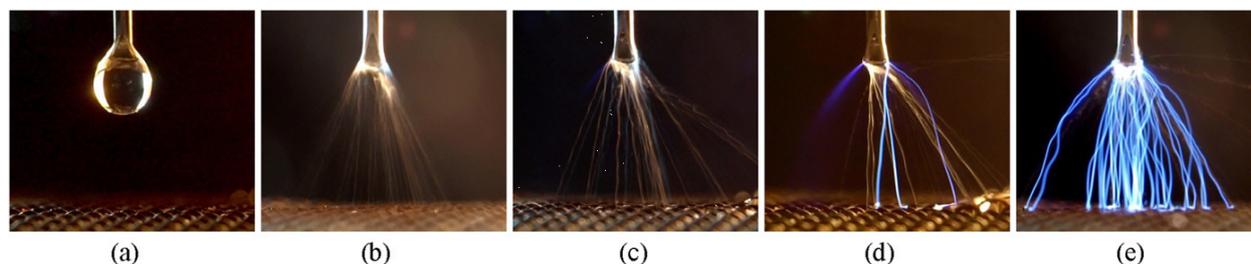
Figure 10. Photographs of the electrospraying of water in 8 mm gap, water flow rate 0.5 ml min^{-1}: (a) droplet without a high voltage, (b) electrospray with a high voltage applied, 5.5 kV, (c) electrospray combined with streamer corona, 6.5 kV, (d) electrospray with transition streamer corona-transient spark, 7.8 kV, (e) electrospray with transient spark, 9 kV. Reproduced from Machala *et al* (2010). © IOP Publishing Ltd. All rights reserved.

10. Future trends for electrospray plasmas

In typical electrospray applications to mass spectroscopy soft ionization, electrospinning, spraying of thin films, nanoparticle production, ink-jet printing, etc, unwanted plasma discharges are prevented by various strategies described in the previous section 8. For example, micro space thrusters trust their robustness and precision on the ability to strictly control the formation of streamers, in particular when large arrays of emitters are at stake (Guerra-García *et al* 2016). On the contrary, in novel areas of applications in water activation for decontamination, plasma medicine and agriculture, or nanoparticle chemical synthesis based on liquid microdroplet irradiation with plasmas, electrosprays are purposely combined with plasma discharges (section 9).

Lietz and Kushner (2016) in numerical modeling showed the importance of the synergy between the plasma and the liquid, including evaporation and the solvation of ions and neutral particles for understanding the outcome of the plasma treatment, and studied the plasma water activation chemical and transport processes on a large dynamic range of timescales. Kruszelnicki *et al* (2017) in their following computational study pointed to the importance of the water microdroplet size (or thin water film thickness) on the transport processes of plasma reactive species into the microdroplets (or thin film). For example, highly soluble species such as H_2O_2 dissolve in water microdroplets readily and deplete their surrounding plasma-gaseous concentration practically independently of the droplet size. On the other hand, the transport of less soluble species such as O_3 or NO_2 into water is strongly limited by the water droplet size (i.e. surface area-limited). These modeling results and very limited current understanding of plasma-liquid interaction processes in this emerging field with its strong application potential will presumably initiate experimental studies of advanced diagnostics of plasma-liquid interactions, including those with electrosprays. However, the complex diagnostic of the processes occurring in the plasma-liquid interface is a great challenge due to the small thickness of this interface and the huge range of timescales involved (Bruggeman *et al* 2016). The strong motivation of these ongoing studies lies in finding the controlling knobs of the water activation in various non-thermal plasma discharges and thus tailoring their application effects by the plasma regime, geometry and the size of the interacting (e.g. electrosprayed) water aerosol droplets.

Consequently, we envision that part of the future trends in this field will go along the exponentially increasing power of numerical simulation, and the necessary physicochemical modelling efforts required to bridge the natural gap and the possible complex landscapes between the molecular and the macroscopic scales numerically resolved. This has already been an increasingly crucial research motivation, applicable in the field of electrospray-assisted processing of materials as it has been the case in the wider research field of surface chemistry in relation to ionic and electric effects. In this endeavor, for example Jusufi *et al* (2009) explored mechanisms like self-assembly assisted by surfactants activated by electric fields using Monte Carlo simulations, while Chu *et al* (2013) reviewed the fundamental role of mesoscopic structures like complex non-spherical micelles (that can be strongly affected by surface electric fields), where the power of numerical simulation was early indicated by Boek *et al* (2002).

Future studies in the field of electrospraying and electrospinning should be focused onto application of various polymers, biomaterials or living cells to biotechnology and to the building of nano- and microstructures for regenerative medicine (Boda *et al* 2018, Bodnár *et al* 2018, Kavadiya and Biswas 2018). However, the effect of electrically generated plasma on the stability of those materials and viability of the cells has not been sufficiently recognized. Mass spectrometry should also be involved to these studies in order to learn about the effect of glow corona or streamer discharges on molecular reactions in electrosprayed or electrospun materials. To those goals, further mass and emission spectroscopy, and microscopic and molecular studies are needed.

11. Conclusions

This review describes the physical processes and phenomena occurring in electrical discharge plasmas combined with electrospraying of liquids, and outlines their potential applications. The phenomenon of electrospraying of liquids by imposing high voltage on the nozzle with the liquid flow has been a subject of many studies for about one century. There are numerous practical applications of this effect, especially in spraying, coating, polymer fiber and textile production by electrospinning, nanoparticle production, and soft ionization of samples for mass spectrometry, besides many others. In most of them, the electrical discharge occurrence, due to high voltage gas ionization, is undesired, since its presence perturbs the stability

J. Phys. D: Appl. Phys. **52** (2019) 233001

Topical Review

of the electrospray. The distorting effect of electrical discharges diminishes for higher liquid flow rates, when the kinetic energy of the jet is very high. Various methods of discharge prevention have been developed, e.g. modification of the electric field in the interelectrode space, increasing the local electric field by reduction of the electrospray nozzle diameter or sharpening its tip, reduction of the conducting surface area of the nozzle, self-controlling the potential at the capillary nozzle, increasing the dielectric strength of the surrounding gas, reduction of the gas pressure or liquid surface tension, or co-axial electrospraying with sheath liquid. In the many papers reviewed, the authors concluded that only the glow corona regime and onset streamers, dependent on the geometry of the liquid meniscus and the jet, do not distort some of the electrospray regimes but, on the contrary, may stabilize the electrospray in the cone-jet mode due to the space charge uniformly distributed around the nozzle tip and the liquid jet.

When, however, the voltage applied to the capillary nozzle is sufficiently high, the streamers produced in the interelectrode space distort the electric field and charge distribution on the liquid surface, and irregular modes of electrospraying occur, which produce larger droplets of polydisperse size distribution. Larger droplets of high electric charge produced in these modes introduce additionally an asymmetry in the electric field that results in off-axis deformation of the liquid meniscus and generation of new droplets in various directions. Although this effect was for a long time considered as unwanted, recently, low temperature plasma produced in electrical discharges of energies higher than in glow corona discharge was employed for water decontamination.

The most typically observed and studied electrical discharges occurring with the electrospray are various modes of corona discharges, especially its glow regime, with significant differences between the polarities. Electrical conductivity and surface tension of the electrosprayed liquid are two key parameters of the electrospraying combined with corona discharge. With increasing surface tension, the voltage required for a stable operation of electrospraying in the cone-jet mode also increases because higher electric field is needed to balance the surface tension force. For liquids of high surface tension (e.g. water) the generation of the cone-jet mode in air is limited by corona discharge, which onsets at the voltage lower than that required for electrospraying. In these combined electrospray-discharge setups, it is non-trivial to distinguish the electrospray current carried by the electrosprayed droplets from the discharge current carried by gaseous ions that is typically much larger. One approach to separate the spray and discharge currents is using grounded coaxial ring electrodes.

One of the key interests in studying the corona discharge in electrosprays is a potential risk of damaging fragile biological samples analysed by mass spectrometry with electrospray ionization. On the other hand, the discharge-induced ionisation can allow for the production of protonated molecules of high proton affinity. Novel plasma-based techniques in ambient air ionization for mass or ion mobility spectrometry, including the low-temperature plasma probe using corona discharge, provide great potential for implementation in stationary or mobile analytical devices.

Optical emission spectroscopy has been widely applied to diagnose electrospray plasmas, especially corona discharges. This method enables characterizing the gas composition, in some cases electron number density from the Stark broadening of H spectral lines and various temperatures, such as electron temperature or gas temperature. All these gas (plasma) parameters, including atomic/molecular concentrations of various species can be determined. In most of the presented studies, liquid electrospray did not significantly influence the emission spectra from the gaseous plasma, unless a high energy discharge would strongly enhance liquid evaporation.

Electrospraying of water combined with various plasma discharges, such as coronas, sparks or dielectric barrier discharges is in focus of numerous recent investigations of atmospheric pressure plasma-liquid interactions and water activation by non-thermal plasma. It brings forth a broad spectrum of potential environmental/biomedical/food/agriculture applications. We also envision that part of the future trends in this field will go along the increasing power of numerical simulations and physicochemical modelling efforts. They will be applicable in the fields of electrospray-assisted processing of materials, surface chemistry, and plasma-liquid interactions in relation to ionic and electric effects.

Acknowledgments

ORCID iDs

Anatol Jaworek ⓘ https://orcid.org/0000-0002-5027-8858
Alfonso M Gañán-Calvo ⓘ https://orcid.org/0000-0002-7552-6184
Zdenko Machala ⓘ https://orcid.org/0000-0003-1424-1350

References

Akazaki M 1965 Corona phenomena from water drops on smooth conductors under high direct voltage *IEEE Trans. Power Appl. Syst.* **84** 1–8

Amad M, Cech N B, Jackson G S and Enke C G 2000 Importance of gas-phase proton affinities in determining the electrospray ionization response for analytes and solvents *J. Mass Spectrom.* **35** 784–9

Andre P, Barinov Y, Faure G, Kaplan V, Lefort A, Shkol'nik S and Vacher D 2001 Experimental study of discharge with liquid non-metallic (tap-water) electrodes in air at atmospheric pressure *J. Phys. D: Appl. Phys.* **34** 3456–65

Anna S L, Bontoux N and Stone H A 2003 Formation of dispersions using 'flow focusing' in microchannels *Appl. Phys. Lett.* **82** 364–6

Asbury G R, Wu C, Siems W F and Hill H H Jr 2000 Separation and identification of some chemical warfare degradation products using electrospray high resolution ion mobility

J. Phys. D: Appl. Phys. 52 (2019) 233001

Topical Review

spectrometry with mass selected detection *Anal. Chim. Acta* **404** 273–83

Baerdemaeker F D, Šimek M and Leys C 2007 Efficiency of hydrogen peroxide production by ac capillary discharge in water solution *J. Phys. D: Appl. Phys.* **40** 2801–9

Bailey A G and Borzabadi E 1978 Natural periodic electrostatic spraying of liquids *IEEE Trans. Ind. Appl.* **14** 162–7

Ballinger K W A, Michelson D and Przybyla J S 1978 The study of the electrical dispersion of dielectric liquids in different gaseous environments *J. Electrostat.* **5** 431–8

Barber P B and Swift D A 1982 A.C. corona discharges and audible noise from water droplets on transmission line conductor *7th Int. Conf. Gas Discharges and their Applications (London, 31 August–3 September 1982)*

Barrero A and Loscertales I G 2007 Micro- and nanoparticles via capillary flows *Annu. Rev. Fluid Mech.* **39** 89–106

Basaran O A 2002 Small-scale free surface flows with breakup: drop formation and emerging applications *AIChE J.* **48** 1842–8

Boda S K, Li X and Xie J 2018 Electrospraying an enabling technology for pharmaceutical and biomedical applications: a review *J. Aerosol Sci.* **125** 164–81

Bodnár E, Grifoll J and Rosell-Llompart J 2018 Polymer solution electrospraying: a tool for engineering particles and films with controlled morphology *J. Aerosol Sci.* **125** 93–118

Boek E S, Jusufi A, Löwen H and Maitland G C 2002 Molecular design of responsive fluids: molecular dynamics studies of viscoelastic surfactant solutions *J. Phys.: Condens. Matter* **14** 9413–30

Borra J P 2006 Nucleation and aerosol processing in atmospheric pressure electrical discharges: powders production, coatings and filtration *J. Phys. D: Appl. Phys.* **39** R19–54

Borra J P 2018 Review on water electro-sprays and applications of charged drops with focus on the corona-assisted cone-jet mode for high efficiency air filtration by wet electro-scrubbing of aerosols *J. Aerosol Sci.* **125** 208–36

Borra J P, Ehouarn P and Boulaud D 2004 Electrohydrodynamic atomisation of water stabilised by glow discharge—operating range and droplet properties *J. Aerosol Sci.* **35** 1313–32

Borra J P, Hartmann R, Marijnissen J and Scarlett B 1996 Destabilisation of sprays in the cone-jet mode by electrical discharges on the jet *J. Aerosol Sci.* **27** S203–4

Borra J P, Tombette Y and Ehouarn P 1999 Influence of electric field profile and polarity on the mode of EHDA related to electric discharge regimes *J. Aerosol Sci.* **30** 913–25

Borra J P, Valt A, Arefi-Khonsari F and Tatoulian M 2012 Atmospheric pressure deposition of thin functional coatings: polymer surface patterning by DBD and post-discharge polymerization of liquid vinyl monomer from surface radicals *Plasma Process. Polym.* **9** 1104–15

Brennan R G, Rabb S A, Jorabchi K, Rutkowski W F and Turk G C 2009 Heat-assisted argon electrospray interface for low-flow rate liquid sample introduction in plasma spectrometry *Anal. Chem.* **81** 8126–33

Bruggeman P and Leys C 2009 Non-thermal plasmas in and in contact with liquids *J. Phys. D: Appl. Phys.* **42** 053001

Bruggeman P and Schram D C 2010 On OH production in water containing atmospheric pressure plasmas *Plasma Sources Sci. Technol.* **19** 045025

Bruggeman P J *et al* 2016 Plasma–liquid interactions: a review and roadmap *Plasma Sources Sci. Technol.* **25** 053002

Bruggeman P, Graham L, Degroote J, Vierendeels J and Leys C 2007 Water surface deformation in strong electrical fields and its influence on electrical breakdown in a metal pin–water electrode system *J. Phys. D: Appl. Phys.* **40** 4779–86

Bruggeman P, Iza F, Guns P, Lauwers D, Kong M G, Gonzalvo Y A, Leys C and Schram D C 2010a Electronic quenching of OH(A) by water in atmospheric pressure plasmas and its influence on the gas temperature determination by OH(A–X) emission *Plasma Sources Sci. Technol.* **19** 015016

Bruggeman P, Liu J, Degroote J, Kong M G, Vierendeels J and Leys C 2008a Dc excited glow discharges in atmospheric pressure air in pin-to-water electrode systems *J. Phys. D: Appl. Phys.* **41** 215201

Bruggeman P, Ribežl E, Maslani A, Degroote J, Malesevic A, Rego R, Vierendeels J and Leys C 2008b Characteristics of atmospheric pressure air discharges with a liquid cathode and a metal anode *Plasma Sources Sci. Technol.* **17** 025012

Bruggeman P, Schram D, Gonzalez M A, Rego R, Kong M G and Leys C 2009 Characterization of a direct dc-excited discharge in water by optical emission spectroscopy *Plasma Sources Sci. Technol.* **18** 025017

Bruggeman P, Verreycken T, Gonzalez M A, Walsh J L, Kong M G, Leys C and Schram D C 2010b Optical emission spectroscopy as a diagnostic for plasmas in liquids: opportunities and pitfalls *J. Phys. D: Appl. Phys.* **43** 124005

Bruins A P 1998 Mechanistic aspects of electrospray ionization *J. Chromatogr.* A **794** 345–57

Burayev T K and Vereshchagin I P 1971 Fizicheskye processy pri rospylenii zhidkostiey v elektricheskom pole *Izv Akad. Nauk SSSR Energ. Transp.* **5** 70–9

Cech N B and Enke C G 2001 Practical implications of some recent studies in electrospray ionization fundamentals *Mass Spectrom. Rev.* **20** 362–87

Chen D-R and Pui D Y H 1997 Experimental investigation of scaling laws for electrospraying: dielectric constant effect *Aerosol Sci. Technol.* **27** 367–80

Chu Z, Dreiss C A and Feng Y 2013 Smart wormlike micelles *Chem. Soc. Rev.* **42** 7174–203

Cloupeau M 1994 Recipes for use of EHD spraying in cone-jet mode and notes on corona discharge effects *J. Aerosol Sci.* **25** 1143–57

Cloupeau M and Prunet-Foch B 1990 Electrostatic spraying of liquids. Main functioning modes *J. Electrostat.* **25** 165–84

Cloupeau M and Prunet-Foch B 1994 Electrohydrodynamic spraying functioning modes. A critical review *J. Aerosol Sci.* **25** 1021–36

Cole R B 2000 Some tenets pertaining to electrospray ionization mass spectrometry *J. Mass Spectrom.* **35** 763–72

Cserfalvi T, Mezei P and Apai P 1993 Emission studies on a glow discharge in atmospheric pressure air using water as a cathode *J. Phys. D: Appl. Phys.* **26** 2184–8

Czech T, Sobczyk A T and Jaworek A 2011 Optical emission spectroscopy of point-plane corona and back-corona discharges in air *Eur. Phys. J.* D **65** 459–74

DePonte D P, Weierstall U, Schmidt K, Warner J, Starodub D, Spence J C H and Doak R B 2008 Gas dynamic virtual nozzle for generation of microscopic droplet streams *J. Phys. D: Appl. Phys.* **41** 195505

Di Natale F, Manna L, La Motta F, Colicchio R, Scaglione E, Pagliuca C and Salvatore P 2018 Capture of bacterial bioaerosol with a wet electrostatic scrubber *J. Electrostat.* **93** 58–68

Dilecce G and De Benedictis S 2011 Laser diagnostics of high-pressure discharges: laser induced fluorescence detection of OH in He/Ar–H_2O dielectric barrier discharges *Plasma Phys. Control. Fusion* **53** 124006

Dole M, Mack L L, Hines R L, Mobley R C, Ferguson L D and Alice M B 1968 Molecular beams of microions *J. Chem. Phys.* **49** 2240–9

Dwivedi P, Matz L M, Atkinson D A and Hill H H Jr 2004 Electrospray ionization-ion mobility spectrometry: a rapid analytical method for aqueous nitrate and nitrite analysis *Analyst* **129** 139–44

Eggers J 1998 Suction power provides a new route to make microdrops *Phys. World* **11** 27

Eggers J and Villermaux E 2008 Physics of liquid jets *Rep. Progr. Phys.* **71** 036601

J. Phys. D: Appl. Phys. **52** (2019) 233001

Topical Review

Elsawah M, Abdel Ghafar H H, Morgan N N, Hassaballah S, Samir A, Elakshar F F and Garamoon A A 2012 Corona discharge with electrospraying system for phenol removal from water *IEEE Trans. Plasma Sci.* **40** 29–34

Elsawah M, Ali M, Hassaballah S, Morgan N, Samir A, Elakshar F and Garamoon A 2013 Wastewater decontamination from microorganisms by electrospraying corona discharge *J. Mod. Phys.* **4** 1632–7

English W N 1948 Corona from a water drop *Phys. Rev.* **74** 179–89

Fantz U 2006 Basics of plasma spectroscopy *Plasma Sources Sci. Technol.* **15** S137–47

Fenn J B, Mann M, Meng C K, Wong S F and Whitehouse C M 1989 Electrospray ionization for mass-spectrometry of large biomolecules *Science* **246** 64–71

Fernandez de la Mora J 2007 The fluid dynamics of Taylor cones *Annu. Rev. Fluid Mech.* **39** 217–43

Fernandez de la Mora J and Gomez A 1993 Remarks on the paper 'generation of micron-sized droplets from the Taylor cone' *J. Aerosol Sci.* **24** 691–5

Fernandez de la Mora J and Loscertales I G 1994 The current emitted by highly conducting Taylor cones *J. Fluid Mech.* **260** 155–84

Forbes T P and Sisco E 2014 Chemical imaging of artificial fingerprints by desorption electro-flow focusing ionization mass spectrometry *Analyst* **139** 2982–5

Forbes T P and Sisco E 2018 Recent advances in ambient mass spectrometry of trace explosives *Analyst* **143** 1948–69

Franzke J 2009 The micro-discharge family (dark, corona, and glow-discharge) for analytical applications realized by dielectric barriers *Anal. Bioanal. Chem.* **395** 549–57

Fridman A and Friedman G 2013 *Plasma Medicine* (New York: Wiley)

Gaisin A F and Son E E 2005 Vapor-air discharges between electrolytic cathode and metal anode at atmospheric pressure *High Temp.* **43** 1–7

Gamero-Castaño M 2010 Energy dissipation in electrosprays and the geometric scaling of the transition region of cone-jets *J. Fluid Mech.* **662** 493–513

Gañán-Calvo A M 1997 On the theory of electrohydrodynamically driven capillary jets *J. Fluid Mech.* **335** 165–88

Gañán-Calvo A M 1998 Generation of steady liquid microthreads and micron- sized monodisperse sprays in gas streams *Phys. Rev. Lett.* **80** 285–8

Gañán-Calvo A M 1999 The surface charge in electrospraying: its nature and its universal scaling laws *J. Aerosol Sci.* **30** 863–72

Gañán-Calvo A M 2004 On the general scaling theory for electrospraying *J. Fluid Mech.* **507** 203–445

Gañán-Calvo A M 2007 Electro-flow focusing: the high-conductivity low-viscosity limit *Phys. Rev. Lett.* **98** 134503

Gañán-Calvo A M and Montanero J M 2009 Revision of capillary cone-jet physics: electrospray and flow focusing *Phys. Rev.* E **79** 066305

Gañán-Calvo A M, Barrero A and Pantano C 1993 The electrohydrodynamics of electrified conical menisci *J. Aerosol Sci.* **24** S19–20

Gañán-Calvo A M, Davila J and Barrero A 1997 Current and droplet size in the electrospraying of liquids. Scaling laws *J. Aerosol Sci.* **28** 249–75

Gañán-Calvo A M, López-Herrera J M and Riesco-Chueca P 2006 The combination of electrospray and flow focusing *J. Fluid Mech.* **566** 421–45

Gañán-Calvo A M, López-Herrera J M, Herrada M A, Ramos A and Montanero J M 2018 Review on the physics of electrospray: from electrokinetics to the operating conditions of single and coaxial Taylor cone-jets, and AC electrospray *J. Aerosol Sci.* **125** 32–56

Gañán-Calvo A M, López-Herrera J M, Rebollo-Muñoz N and Montanero J M 2016 The onset of electrospray: the universal scaling laws of the first ejection *Sci. Rep.* **6** 32357

Garstecki P, Gañán-Calvo A M and Whitesides G M 2005 Formation of bubbles and droplets in microfluidic systems *Bull. Pol. Acad. Sci.* **53** 361–72

Gemci T, Hitron R and Chigier N 2002 Measuring charge-to-mass ratio of individual droplets using phase Doppler interferometery *ILASS Americas, 15th Ann. Conf. Liquid Atomization and Spray Systems (Madison, WI, May 2002)* pp 241–5

Giao T N and Jordan J B 1968 Modes of corona discharge in air *IEEE Trans. Power App. Syst.* **87** 1207–15

Guerra-García C, Krejci D and Lozano P 2016 Spatial uniformity of the current emitted by an array of passively fed electrospray porous emitters *J. Phys. D: Appl. Phys.* **49** 115503

Hara M and Akazaki M 1981 Onset mechanism and development of corona discharge on water drops dripping from a conductor under high direct voltage *J. Electrostat.* **6** 339–53

Hara M, Ishibe S and Akazaki M 1979 Corona discharge and electrical charge on water drops dripping from d.c. transmission conductors—an experimental study in laboratory *J. Electrostat.* **6** 235–57

Hara M, Ishibe S, Sumiyoshitani S and Akazaki M 1980 Electrical corona and specific charge on water drops from a cylindrical conductor with high d.c. voltage *J. Electrostat.* **6** 239–70

Harmann G 1984 Theoretical evaluation of Peek's law *IEEE Trans. Ind. Appl.* **20** 1647–51

Hartman R P A, Brunner D J, Camelot D M A, Marijnissen J C M and Scarlett B 1999 Electrohydrodynamic atomization in the cone-jet mode. Physical modeling of the liquid cone and jet *J. Aerosol Sci.* **30** 823–49

Hayati I, Bailey A I and Tadros T F 1986 Mechanism of stable jet formation in electrohydrodynamic atomization *Nature* **319** 41–2

Hayati I, Bailey A I and Tadros T F 1987a Investigations into the mechanisms of electrohydrodynamic spraying of liquids: I. Effect of electric field and the environment on pendant drop and factors affecting the formation of stable jets and atomization *J. Coll. Interface Sci.* **117** 205–21

Hayati I, Bailey A I and Tadros T F 1987b Investigations into the mechanisms of electrohydrodynamic spraying of liquids: II. Mechanism of stable jet formation and electrical forces acting on a liquid cone *J. Coll. Interface Sci.* **117** 222–30

Higashiyama Y, Nakajima T and Sugimoto T 2017 Influence of conductivity on corona discharge current from a water droplet and on ejection of nano-sized droplets *J. Electrostat.* **88** 65–70

Higuera F J 2010 Numerical computation of the domain of operation of an electrospray of a very viscous liquid *J. Fluid Mech.* **648** 35–52

Hoburg J F and Melcher J R 1975 Current-driven, corona-terminated water jets as a source of charged droplets and audible noise *IEEE Trans. Power Appar. Syst.* **94** 128–36

Hong Y C, Huh J Y, Ma S H and Kim K I 2018 Inactivation of microorganisms by radical droplets from combination of water discharge and electro-spraying *J. Electrost.* **91** 56–60

Huber C G and Krajete A 2000 Sheath liquid effects in capillary high-performance liquid chromatography—electrospray mass spectrometry of oligonucleotides *J. Chromatogr.* A **870** 413–24

Hulthe G, Stenhagen G, Wennerström O and Ottosson C H 1997 Water clusters studied by electrospray mass spectrometry *J. Chromatogr.* A **777** 155–65

Ijsebaert J C, Geerse K B, Marijnissen J C M and Scarlett B 1999 Electrohydrodynamic spraying of inhalation medicine *J. Aerosol Sci.* **30** 825–6

Ijsebaert J C, Geerse K B, Marijnissen J C M, Lammers J W J and Zanen P 2001 Electro-hydrodynamic atomization of drug solutions for inhalation purposes *J. Appl. Physiol.* **91** 2735–41

Ikonomou M G, Blades A T and Kebarle P 1991 Electrospray mass spectrometry of methanol and water solutions suppression of electric discharge with SF_6 gas *J. Am. Soc. Mass Spectrom.* **2** 497–505

J. Phys. D: Appl. Phys. **52** (2019) 233001

Topical Review

Jackson G S and Enke C G 1999 Electrical equivalence of electrospray ionization with conducting and nonconducting needles *Anal. Chem.* **71** 3777–84

Jaworek A and Krupa A 1996a Generation and characteristics of the precession mode of EHD spraying *J. Aerosol Sci.* **27** 75–82

Jaworek A and Krupa A 1996b Forms of the multijet mode of electrohydrodynamic spraying *J. Aerosol Sci.* **27** 979–86

Jaworek A and Krupa A 1997 Studies of the corona discharge in ehd spraying *J. Electrostat.* **40–1** 173–8

Jaworek A and Krupa A 1999a Classification of the modes of EHD spraying *J. Aerosol Sci.* **30** 873–93

Jaworek A and Krupa A 1999b Jet and drop formation in electrohydrodynamic spraying of liquids. A systematic approach *Exp. Fluids* **27** 43–52

Jaworek A, Czech T, Rajch E and Lackowski M 2005 Spectroscopic studies of electric discharges in electrospraying *J. Electrostat.* **63** 635–41

Jaworek A, Sobczyk A T and Krupa A 2018 Electrospray application to powder production and surface coating *J. Aerosol Sci.* **125** 57–92

Jaworek A, Sobczyk A T, Czech T and Krupa A 2014 Corona discharge in electrospraying *J. Electrostat.* **72** 166–78

Jaworek A, Sobczyk A T, Krupa A, Marchewicz A, Krella A K and Czech T 2016 Thin films by EHDA. A review *Int. J. Plasma Environ. Sci. Technol.* **10** 29–34

Joffre G H and Cloupeau M 1986 Characteristic forms of electrified menisci emitting charges *J. Electrostat.* **18** 147–61

Jung J-S, Moon J-D, Kim J-G and Geum S-T 2009 EHD atomization characteristics of a point-plate system with a porous point electrode *J. Electrostat.* **67** 862–9

Jusufi A, Hynninen A-P, Haataja M and Panagjotopoulos A Z 2009 Electrostatic screening and charge correlation effects in micellization of ionic surfactants *J. Phys. Chem.* B **113** 6314–20

Kanazawa S, Hirao M, Kocik M and Mizeraczyk J 2009 Time resolved imaging of pulsed streamer discharge at the air/water interface *J. Plasma Fusion Res. Ser.* **8** 615–8

Kanazawa S, Kawano H, Watanabe S, Furuki T, Akamine S, Ichiki R, Ohkubo T, Kocik M and Mizeraczyk J 2011 Observation of OH radicals produced by pulsed discharges on the surface of a liquid *Plasma Sources Sci. Technol.* **20** 034010

Kanazawa S, Tanaka H, Kujiwara A, Ohkubo T, Nomoto Y, Kocik M, Mizeraczyk J and Chang J S 2007 LIF imaging of OH radicals in DC positive streamer coronas *Thin Solid Films* **515** 4266–71

Kavadiya S and Biswas P 2018 Electrospray deposition of biomolecules: applications, challenges, and recommendations *J. Aerosol Sci.* **125** 182–207

Kawamoto H, Umezu S and Koizumi R 2005 Fundamental investigation on electrostatic ink jet phenomena in pin-to-plate discharge system *J. Imaging Sci. Technol.* **49** 19–27

Kebarle P 2000 A brief overview of the present status of the mechanisms involved in electrospray mass spectrometry *J. Mass Spectrom.* **35** 804–17

Kim H J, Lee J H, Kim M Y, Cerfalvi T and Mezei P 2000 Development of open-air type electrolyte-as-cathode glow discharge-atomic emission spectrometry for determination of trace metals in water *Spectrochim. Acta* B **55** 823–31

Kim H-H, Kim J-H and Ogata A 2011 Time-resolved high-speed camera observation of electrospray *J. Aerosol Sci.* **42** 249–63

Kim H-H, Teramoto Y, Negishi N, Ogata A, Kim J H, Pongrác B, Machala Z and Gañán-Calvo A M 2014 Polarity effect on the electrohydrodynamic (EHD) spray of water *J. Aerosol Sci.* **76** 98–114

Kim M C and Lee S Y 2004 Change of atomization performance with selection of nozzle materials in electrohydrodynamic spraying *At. Sprays* **14** 175–90

Kiontke A, Engel C, Belder D and Birkemeyer C 2018a Analyte and matrix evaporability—key players of low-temperature plasma ionization for ambient mass spectrometry *Anal. Bioanal. Chem.* **410** 5123–30

Kiontke A, Holzer F, Belder D and Birkemeyer C 2018b The requirements for low-temperature plasma ionization support miniaturization of the ion source *Anal. Bioanal. Chem.* **410** 3715–22

Klee S, Thinius T, Brockmann K J and Benter T 2014 Capillary atmospheric pressure chemical ionization using liquid point electrodes *Rapid Commun. Mass Spectrom.* **28** 1591–600

Kordova T, Scholtz V, Khun J, Souskova H, Hozak P and Cerovsky M 2018 Inactivation of microbial food contamination of plastic cups using nonthermal plasma and hydrogen peroxide *J. Food Qual.* **2018** 5616437

Korkut S, Saville D A and Aksay I A 2008 Enhanced stability of electrohydrodynamic jets through gas ionization *Phys. Rev. Lett.* **100** 034503

Kovalova Z, Leroy M, Kirkpatrick M J, Odic E and Machala Z 2016 Corona discharges with water electrospray for *Escherichia coli* biofilm eradication on a surface *Bioelectrochemistry* **112** 91–9

Kovalova Z, Tarabova K, Hensel K and Machala Z 2013 Decontamination of *Streptococci* biofilms and *Bacillus cereus* spores on plastic surfaces with DC and pulsed corona discharges *Eur. Phys. J. Appl. Phys.* **61** 24306

Kruszelnicki J, Lietz A M and Kushner M J 2017 Interaction between atmospheric pressure plasmas and liquid micro-droplets *Conf. Program and Book of Abstracts, Int. Conf. on Plasmas with Liquids (ICPL 2017)* ed P Lukeš and K Koláček (Prague: Institute of Plasma Physics CAS) p 37

Ku B K and Kim S S 2002 Electrospray characteristics of highly viscous liquids *J. Aerosol Sci.* **33** 1361–78

Ku B K and Kim S S 2003 Electrohydrodynamic spraying characteristics of glycerol solutions in vacuum *J. Electrostat.* **57** 109–28

Kuroda S and Horiuchi T 1984 Effects of corona discharge of the formation of electrically-extracted liquid jets *Japan. J. Appl. Phys.* **23** 1598–607

Lamarche C, Da Silva C, Demol G, Dague E, Rols M-P and Pillet F 2018 Electrical discharges in water induce spores' DNA damage *PLoS One* **13** e0201448

Laroussi M, Kong M G, Morfill G and Stolz W 2012 *Plasma Medicine: Applications of Low-Temperature Gas Plasmas in Medicine and Biology* (Cambridge: Cambridge University Press) (https://doi.org/10.1017/CBO9780511902598)

Lastochkin D and Chang H-C 2005 A high-frequency electrospray driven by gas volume charges *J. Appl. Phys.* **97** 123309

Laux C O, Spence T G, Kruger C H and Zare R N 2003 Optical diagnostics of atmospheric pressure air plasmas *Plasma Sources Sci. Technol.* **12** 125–38

Lenggoro I W and Okuyama K 1997 Preparation of nanometer-sized zinc sulfide particles by electrospray pyrolysis *J. Aerosol Sci.* **28** S351–2

Lenggoro I W, Okuyama K, Fernandez de la Mora J and Tohge N 2000 Preparation of ZnS nanoparticles by electrospray pyrolysis *J. Aerosol Sci.* **31** 121–36

Lenggoro I W, Xia B, Okuyama K and Fernandez de la Mora J 2002 Sizing of colloidal nanoparticles by electrospray and differential mobility analyzer methods *Langmuir* **18** 4584–91

Lietz A M and Kushner M J 2016 Air plasma treatment of liquid covered tissue: long timescale chemistry *J. Phys. D: Appl. Phys.* **49** 425204

Liu F, Wang W, Wang S, Zheng W and Wang Y 2007 Diagnostic of OH radical by optical emission spectroscopy in wire-plate bi-directional pulsed corona discharge *J. Electrostat.* **65** 445–51

J. Phys. D: Appl. Phys. **52** (2019) 233001

Topical Review

Liu F, Wang W, Zheng W and Wang Y 2008 Investigation of spatially resolved spectra of OH and N_2^+ in N_2 and H_2O mixture wire-plate positive pulsed streamer discharge *Spectrochim. Acta* A **69** 776–81

Locke B R and Shih K-Y 2011 Review of the methods to form hydrogen peroxide in electrical discharge plasma with liquid water *Plasma Sources Sci. Technol.* **20** 034006

Lopez-Herrera J M, Barrero A, Boucard A, Loscertales I G and Marquez M 2004 An experimental study of the electrospraying of water in air at atmospheric pressure *J. Am. Soc. Mass Spectrom.* **15** 253–9

Lopez-Herrera J M, Barrero A, Lopez A, Loscertales I G and Marquez M 2003 Coaxial jets generated from electrified Taylor cones. Scaling laws *J. Aerosol Sci.* **34** 535–52

Loscertales I G, Barrero A, Guerrero I, Cortijo R, Marquez M and Gañán-Calvo A M 2002 Micro/nano encapsulation via electrified coaxial liquid jets *Science* **295** 1695–8

Lukes P, Locke B R and Brisset J L 2012 Aqueous-phase chemistry of electrical discharge plasma in water and in gas–liquid environments *Plasma Chemistry and Catalysis in Gases and Liquids* ed V I Parvulescu *et al* (Weinheim: Wiley) (https://doi.org/10.1002/9783527649525)

Machala Z, Chládeková L and Pelach M 2010 Plasma agents in bio-decontamination by dc discharges in atmospheric air *J. Phys. D: Appl. Phys.* **43** 222001

Machala Z, Hensel K and Akishev Y 2012 *Plasma for Bio-Decontamination, Medicine and Food Security* (*NATO Science for Peace and Security Series A: Chemistry and Biology*) (Berlin: Springer)

Machala Z, Janda M, Hensel K, Jedlovsky I, Leštinská L, Foltin V, Martišovitš V and Morvová M 2007 Emission spectroscopy of atmospheric pressure plasmas for bio-medical and environmental applications *J. Mol. Spectrosc.* **243** 194–201

Machala Z, Jedlovsky I and Martišovitš V 2008 DC discharges in atmospheric air and their transitions *IEEE Trans. Plasma Sci.* **36** 918–9

Machala Z, Jedlovsky I, Chladekova L, Pongrac B, Giertl D, Janda M, Šikurova L and Polčic P 2009 DC discharges in atmospheric air for bio-decontamination—spectroscopic methods for mechanism identification *Eur. Phys. J.* D **54** 195–204

Machala Z, Tarabova B, Hensel K, Spetlikova E, Sikurova L and Lukes P 2013 Formation of ROS and RNS in water electro-sprayed through transient spark discharge in air and their bactericidal effects *Plasma Process. Polym.* **10** 649–59

Machala Z, Tarabova B, Sersenova D, Janda M and Hensel K 2019 Chemical and antibacterial effects of plasma activated water: correlation with gaseous and aqueous reactive oxygen and nitrogen species, plasma sources and air flow conditions *J. Phys. D: Appl. Phys.* **52** 034002

Macky W A 1931 Some investigations on the deformation and breaking of water drops in strong electric field *Proc. R. Soc.* A **133** 565–87

Maguire P *et al* 2015 Controlled microdroplet transport in an atmospheric pressure microplasma *Appl. Phys. Lett.* **106** 224101

Maguire P, Rutherford D, Macias-Montero M, Mahony C, Kelsey C, Tweedie M, Pérez-Martin F, McQuaid H, Diver D and Mariotti D 2017 Continuous in-flight synthesis for on-demand delivery of ligand-free colloidal gold nanoparticles *Nano Lett.* **17** 1336–43

Matz L M, Clowers B H, Steiner W E, Siems W F and Hill H H Jr 2001 Liquid-sheath-flow electrospray ionization feasibility study of direct water analysis with the use of high-resolution ion-mobility spectrometry *Field Anal. Chem. Technol.* **5** 91–6

McQuinn K, Hof F and McIndoe J S 2007 Direct observation of ion evaporation from a triply charged nanodroplet *Chem. Commun.* **2007** 4099–101

McQuinn K, Hof F and McIndoe J S 2009 Collision-induced dissociation of protonated nanodroplets *Int. J. Mass Spectrom.* **279** 32–6

Meesters G M H, Vercoulen P H W, Marijnissen J C M and Scarlett B 1991 A sub-micron aerosol generator, using a high electric field *J. Aerosol Sci.* **22** S11–4

Meesters G M H, Vercoulen P H W, Marijnissen J C M and Scarlett B 1992 Generation of micron-sized droplets from the Taylor cone *J. Aerosol Sci.* **23** 37–49

Melcher J R and Taylor G I 1969 Electrohydrodynamics: a review of the role of interfacial shear stresses *Annu. Rev. Fluid Mech.* **1** 111–47

Metelmann H R, von Woedtke T and Weltmann K-D 2018 *Comprehensive Clinical Plasma Medicine* (Berlin: Springer)

Mezei P, Cserfalvi T and Csillag L 2005 The spatial distribution of the temperatures and the emitted spectrum in the electrolyte cathode atmospheric glow discharge *J. Phys. D: Appl. Phys.* **38** 2804–11

Mezei P, Cserfalvi T, Kim H J and Mottaleb M A 2001 The influence of chlorine on the intensity of metal atomic lines emitted by an electrolyte cathode atmospheric glow discharge *Analyst* **126** 712–4

Motyka A, Dzimitrowicz A, Jamroz P, Lojkowska E, Sledz W and Pohl P 2017 Rapid eradication of bacterial phytopathogens by atmospheric pressure glow discharge generated in contact with a flowing liquid cathode *Biotechnol. Bioeng.* **115** 1581–93

Ogata S, Hara Y and Shinohara H 1978 The break-up mechanism of a charged liquid jet *Int. Chem. Eng.* **18** 482–8

Ohkubo T, Kanazawa S, Nomoto Y, Kocik M and Mizeraczyk J 2005 Characteristics of DC corona streamers induced by UV laser irradiation in non-thermal plasma *J. Adv. Oxid. Technol.* **8** 218–25

Pantano C, Gañán-Calvo A M and Barrero A 1994 Zeroth-order, electrohydrostatic solution for electrospraying in cone-jet mode *J. Aerosol Sci.* **25** 1065–77

Pareta R, Brindley A, Edirisinghe M J, Jayasinghe S N and Luklinska Z B 2005 Electrohydrodynamic atomization of protein (bovine serum albumin) *J. Mater. Sci., Mater. Med.* **16** 919–25

Park H, Kim K and Kim S 2004 Effects of a guard plate on the characteristics of an electrospray in the cone-jet mode *J. Aerosol Sci.* **35** 1295–312

Park I, Hong W S, Kim S B and Kim S S 2017 Experimental investigations on characteristics of stable water electrospray in air without discharge *Phys. Rev.* E **95** 063110

Pearse R W B and Gaydon A G 1963 *The Identification of Molecular Spectra* (London: Chapman and Hall)

Phan-Cong J L, Pirotte P, Brunelle R and Giao Trinh N 1974 A study of corona discharges at water drops over the freezing temperature range *IEEE Trans. Power Appar. Syst.* **93** 727–34

Pieterse C L 2013 Electrohydrodynamic atomization limitations at atmospheric conditions due to corona discharge *IEEE EUROCON Conf. (Zagreb, Croatia, 1–4 July 2013)* ed I Kuzle *et al* pp 1897–903

Pieterse C L, Papka P and Perold W J 2015 Polarization and corona discharge threshold field calculation of electrospraying point-to-plane geometries *J. Electrostat.* **75** 104–15

Poncelet D, Neufeld R J, Goosen M F A, Bugarski B and Babak V 1999 Formation of microgel beads by electric dispersion of polymer solutions *AIChE J.* **45** 2018–23

Ponce-Torres A, Rebollo-Muñoz N, Herrada M A, Gañán-Calvo A M and Montanero J M 2018 The steady cone-jet mode of electrospraying close to the minimum volume stability limit *J. Fluid Mech.* **857** 142–72

Pongrac B and Machala Z 2011 Electrospraying of water with streamer corona discharge *IEEE Trans. Plasma Sci.* **39** 2664–5

Pongrac B, Kim H-H, Janda M, Martisovits V and Machala Z 2014a Fast imaging of intermittent electrospraying of water with positive corona discharge *J. Phys. D: Appl. Phys.* **47** 315202

J. Phys. D: Appl. Phys. **52** (2019) 233001

Topical Review

Pongrac B, Kim H-H, Negishi N and Machala Z 2014b Influence of water conductivity on particular electrospray modes with dc corona discharge—optical visualization approach *Eur. Phys. J.* D **68** 224

Pongrac B, Krcma F, Dostal L, Kim H-H, Homola T and Machala Z 2016 Effects of corona space charge polarity and liquid phase ion mobility on the shape and velocities of water jets in the spindle jet and precession modes of water electro-spray *J. Aerosol Sci.* **101** 196–206

Puač N, Gherardi M and Shiratani M 2017 Plasma agriculture: a rapidly emerging field *Plasma Process. Polym.* **15** e1700068

Pyrgiotakis G, McDevitt J, Yamauchi T and Demokritou P 2012 A novel method for bacterial inactivation using electrosprayed water nanostructures *J. Nanopart. Res.* **14** 1027

Pyrgiotakis G, Vedantam P, Cirenza C, McDevitt J, Eleftheriadou M, Leonard S S and Demokritou P 2016 Optimization of a nanotechnology based antimicrobial platform for food safety applications using engineered water nanostructures (EWNS) *Sci. Rep.* **6** 21073

Rosell-Llompart J and Fernandez de la Mora J 1994 Generation of monodisperse droplets 0.3–4 μm in diameter from electrified cone-jets of highly conducting and viscous liquids *J. Aerosol Sci.* **25** 1093–119

Sabo M and Matejcik S 2012 Corona discharge ion mobility spectrometry with orthogonal acceleration time of flight mass spectrometry for monitoring of volatile organic compounds *Anal. Chem.* **84** 5327–34

Sabo M, Malaskova M, Harmathova O, Hradski J, Masar M, Radjenovic B and Matejcik S 2015 Direct liquid sampling for corona discharge ion mobility spectrometry *Anal. Chem.* **87** 7389–94

Saville D A 1997 Electrohydrodynamics: the Taylor–Melcher leaky dielectric model *Annu. Rev. Fluid Mech.* **29** 27–64

Schultze K 1961 Das Verhalten verschiedener Flüssigkeiten bei der Elektrostatischen Zerstaubung *Z. Angew. Phys.* **13** 11–6

Sember V 2002 Spectroscopic measurement of temperature and composition of a plasma jet generated by a hybrid water argon arc torch *Czech. J. Phys.* **52** D643–50

Shirai N, Ichinose K, Uchida S and Tochikubo F 2011a Influence of liquid temperature on the characteristics of an atmospheric DC glow discharge using a liquid electrode with a miniature helium flow *Plasma Sources Sci. Technol.* **20** 034013

Shirai N, Matsui K, Ibuka S and Ishii S 2011b Atmospheric negative corona discharge observed at tip of Taylor cone using PVA solution *IEEE Trans. Plasma Sci.* **39** 2210–1

Shirai N, Nakazawa M, Ibuka S and Ishii S 2012 Generation and control of electrolyte cathode atmospheric glow discharge using miniature gas flow *Electr. Eng. Japan* **178** 8–15

Shirai N, Onaka Y, Ibuka S and Ishii S 2008 Formation of ethanol filament and its pulsed discharge for microplasma generation *Japan. J. Appl. Phys.* **47** 2244–9

Shirai N, Onaka Y, Ibuka S, Yasuoka K and Ishii S 2007 Generation of microplasma using pulsed discharge of ethanol droplet in air *Japan. J. Appl. Phys.* **46** 370–4

Shirai N, Sekine R, Uchida S and Tochikubo F 2014 Atmospheric negative corona discharge using Taylor cone as a liquid cathode *Japan. J. Appl. Phys.* **53** 026001

Shmelev V 2008 Propagation modes of an electrical discharge along a liquid jet *IEEE Trans. Plasma Sci.* **36** 2522–7

Shmelev V, Saveliev A V and Kennedy L A 2009 Plasma chemical reactor with exploding water jet *Plasma Chem. Plasma Process.* **29** 275–90

Shorey J D and Michelson D 1970 On the mechanism of electrospraying *Nucl. Instrum. Methods Phys. Res.* **82** 295–6

Sjöberg P J R, Nyholm L and Markides K E 2000 Characterization of atmospheric pressure ionization mass spectrometric process obtained using a fused-silica emitter with the high voltage applied upstream *J. Mass Spectrom.* **35** 330–6

Skarja M, Berden M and Jerman I 1998 Influence of ionic composition of water on the corona discharge around water drops *J. Appl. Phys.* **84** 2436–42

Smith D P H 1986 The electrohydrodynamic atomization of liquids *IEEE Trans. Ind. Appl.* **22** 527–35

Smith D R and Wood T D 2003 Graphite-coated nanoelectrospray emitter for mass spectrometry *Anal. Chem.* **75** 7015–9

Stewart I I 1999 Electrospray mass spectrometry: a tool for elemental speciation *Spectrochim. Acta* B **54** 1649–95

Stommel Y G, Kirchhoff M and Riebel U 2006 Experimental results on the influence of concentrated liquid aerosols on the onset voltage of corona discharge *J. Electrostat.* **64** 836–42

Straub R F and Voyksner R D 1993 Negative ion formation in electrospray mass spectrometry *J. Am. Soc. Mass Spectrom.* **4** 578–87

Sugama C, Tochikobo F and Uchida S 2006 Glow discharge formation over water surface at saturated water vapor pressure and its application to wastewater treatment *Japan. J. Appl. Phys.* **45** 8858–63

Sugimoto T, Asano K and Higashiyama Y 2001 Negative corona discharge at a tip of water cone deformed under dc field *J. Electrostat.* **53** 25–38

Sun B, Sato M and Clements J S 1997 Optical study of active species produced by a pulsed streamer corona discharge in water *J. Electrostat.* **39** 189–202

Sun B, Sato M, Harano A and Clements J S 1998 Non-uniform pulse discharge-induced radical production in distilled water *J. Electrostat.* **43** 115–26

Šunka P, Babicky V, Člupek M, Lukeš P, Šimek M, Schmidt J and Černak M 1999 Generation of chemically active species by electrical discharges in water *Plasma Sources Sci. Technol.* **8** 258–65

Tang K and Gomez A 1994 Generation by electrospray of monodisperse water droplets for targeted drug delivery by inhalation *J. Aerosol Sci.* **25** 1237–49

Tang K and Gomez A 1995 Generation of monodisperse water droplets from electrosprays in a corona-assisted cone-jet mode *J. Coll. Interface Sci.* **175** 326–32

Tatoulian M, Arefi-Khonsari F, Tatoulian L, Amouroux J and Borra J P 2006 Deposition of poly(acrylic acid) films by electrohydrodynamic atomization in postdischarge at atmospheric pressure in air *Chem. Mater.* **18** 5860–3

Teer D and Dole M 1975 Electrospray mass spectroscopy of macromolecule degradation in the electrospray *J. Polym. Sci.* **13** 985–95

Thirumdas R, Kothakota A, Annapure U, Siliveru K, Blundell R, Gatt R and Valdramidis V P 2018 Plasma activated water (PAW): chemistry, physico-chemical properties, applications in food and agriculture *Trends Food Sci. Technol.* **77** 21–31

Thundat T, Warmack R J, Allison D P and Ferrell T L 1992 Electrostatic spraying of DNA molecules for investigating by scanner tunnelling microscopy *Ultramicroscopy* **42–4** 1083–7

Townsend J S 1914 The potentials required to maintain currents between coaxial cylinders *Phil. Mag.* **28** 83–90

Uematsu I, Matsumoto H, Morota K, Minagawa M, Tanioka A, Yamagata Y and Inoue K 2004 Surface morphology and biological activity of protein thin films produced by electrospray deposition *J. Colloid Interface Sci.* **269** 336–40

Vaze N D, Park S, Brooks A D, Fridman A and Joshi S G 2017 Involvement of multiple stressors induced by non-thermal plasma-charged aerosols during inactivation of airborne bacteria *PLoS One* **12** e0171434

Wampler F M III, Blades A T and Kebarle P 1993 Negative ion electrospray mass spectrometry of nucleotides: ionization from water solution with SF_6 discharge suppression *J. Am. Soc. Mass Spectrom.* **4** 289–95

Wróblewski T, Gazda E, Mechlińska-Drewko J and Karwasz G P 2001 Swarm experiment on ionized water clusters *Int. J. Mass Spectrom.* **207** 97–110

J. Phys. D: Appl. Phys. **52** (2019) 233001

Topical Review

Wróblewski T, Ziemczonek L, Gazda E and Karwasz G P 2003 Dissociation energies of protonated water clusters *Radiat. Phys. Chem.* **68** 313–8

Xiao P and Staak D 2014 Microbubble generation by microplasma in water *J. Phys. D: Appl. Phys.* **47** 355203

Xu P, Zhang B, Wang Z, Chen S and He J 2017 Dynamic corona characteristics of water droplets on charged conductor surface *J. Phys. D: Appl. Phys.* **50** 085201

Xu Y, Skotak M and Hanna M 2006 Electrospray encapsulation of water-soluble protein with polylactide. I. Effects of formulations and process on morphology and particle size *J. Microencapsul.* **23** 69–78

Yamashita M and Fenn J B 1984 Negative ion production with the electrospray ion source *J. Phys. Chem.* **88** 4671–5

Yuill E M, Shi W, Poehlman J and Baker L A 2015 Scanning electrospray microscopy with nanopipets *Anal. Chem.* **87** 11182–6

Yurteri C U, Hartman R P A and Marijnissen J C M 2010 Producing pharmaceutical particles via electrospraying with an emphasis on nano and nano structured particles—a review *KONA Powder Part. J.* **28** 91–115

Zeleny J 1914 The electrical discharge from liquid points and a hydrostatic method of measuring the electric intensity at their surfaces *Phys. Rev.* **3** 69–91

Zeleny J 1915 On the conditions of instability of electrified drops with applications to the electrical discharge from liquid points *Proc. Camb. Phil. Soc.* **18** 71–83

Zeleny J 1917 Instability of electrified liquid surface *Phys. Rev.* **10** 1–6

Zeleny J 1920 Electrical discharges from pointed conductors *Phys. Rev.* **16** 102–25

Zhou S and Cook K D 2000 Protonation in electrospray mass spectrometry: wrong-way-round or right-way-round? *J. Am. Soc. Mass Spectrom.* **11** 961–6